CHAPTER 4

Advanced Catalyst Design in the Oxidative Kinetic Resolution

4.1 Background and Introduction

The development of improved catalysts for the oxidative kinetic resolution of secondary alcohols is critical to the enhanced utility of this process. Better catalysts provide more selective oxidations of a broader range of substrates in shorter reaction times, while maximizing the operational simplicity and safety of the transformation. Thus, the exploration of alternative systems for the aerobic enantioselective oxidation of secondary alcohols is of great value.[1]

Initial efforts in the area of enantioselective alcohol oxidation were based on the mild aerobic oxidation reported by Uemura.[2] Eric Ferreira, a graduate student in these laboratories, discovered that the use of the commercially available diamine (–)-sparteine (**28**) as a chiral additive with $Pd(OAc)_2$ under an atmosphere of molecular oxygen could provide kinetic resolution of (±)-1-phenylethanol ((±)-**25**), albeit in low conversion and with modest selectivity (Scheme 4.1.1).[3,4]

Scheme 4.1.1 Resolution with (–)-sparteine and $Pd(OAc)_2$.

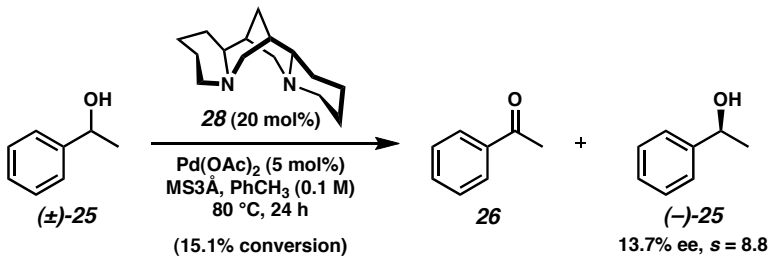

Catalyst modification was aided by an investigation of the mechanism for the oxidation, as proposed by Uemura (Scheme 4.1.2).[2b] Throughout the catalytic cycle, from initial alcohol coordination to form palladium alkoxide **228**, to subsequent β-

hydride elimination to form palladium hydride **229**, and to reaction with molecular oxygen to generate palladium peroxide **230**, counterion X is coordinated to the metal center. It was proposed that varying this counterion by changing the palladium catalyst precursor would have a marked effect on the reactivity and the selectivity of the system.

Scheme 4.1.2 Proposed mechanistic role of counterion.

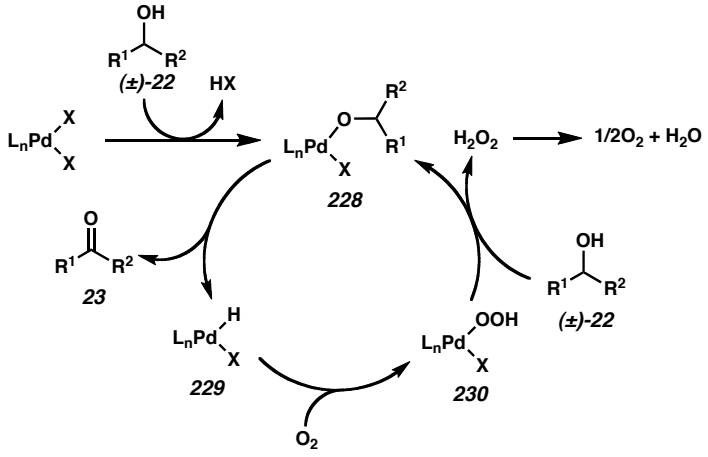

Indeed, this reaction displays a strong catalyst counterion dependence (Table 4.1.1). A palladium(0) precursor (entry 2), in which the counterion in presumed palladium(II) intermediates **228**, **229**, and **230** are not clear, provided reasonable levels of oxidation but decreased selectivity. Palladium precursors with chloride counterions (entries 3 and 4) led to more reactive and selective catalyst systems than those with acetate (entry 1), with $Pd(nbd)Cl_2$ emerging as the most effective palladium source. Interestingly, the use of a palladium bromide source (entry 5) led to rapid palladium aggregation and little oxidation.[5]

Table 4.1.1 Palladium source screen in toluene.

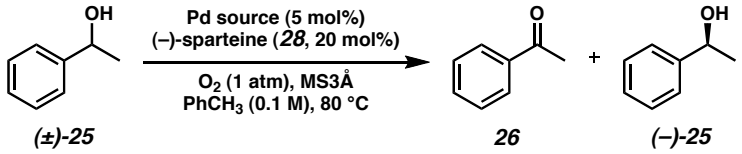

(±)-25 *26* *(–)-25*

entry	Pd source	time	conversion[a]	alcohol ee[b]	*s*
1	$Pd(OAc)_2$	24 h	15.1%	13.7%	8.8
2	$Pd_2(dba)_3$	55 h	66.2%	81.5%	5.7
3	$PdCl_2$	96 h	62.6%	98.0%	16
4	$Pd(nbd)Cl_2$	96 h	59.9%	98.7%	23
5[c]	$PdBr_2$	60 h	5.4%	5.0%	16

[a] Measured by GC. [b] Measured by chiral HPLC. [c] Pd black observed.

Theoretical calculations by the Goddard group confirmed the importance of the counterion for selectivity in the resolution.[6] The rate-limiting step in the catalytic cycle was found to be β-hydride elimination from the palladium alkoxide intermediate.[7] The counterion has a critical role imparting stereoselectivity to the process by occupying an open apical position in the β-hydride elimination transition state (Figure 4.1.1). Calculations correctly predicted the observed selectivity difference between larger chloride and smaller acetate counterions. Additionally, little selectivity (s = 1.5) was anticipated in the absence of a counterion.

Figure 4.1.1 Theoretical calculations on the enantioselective oxidation.

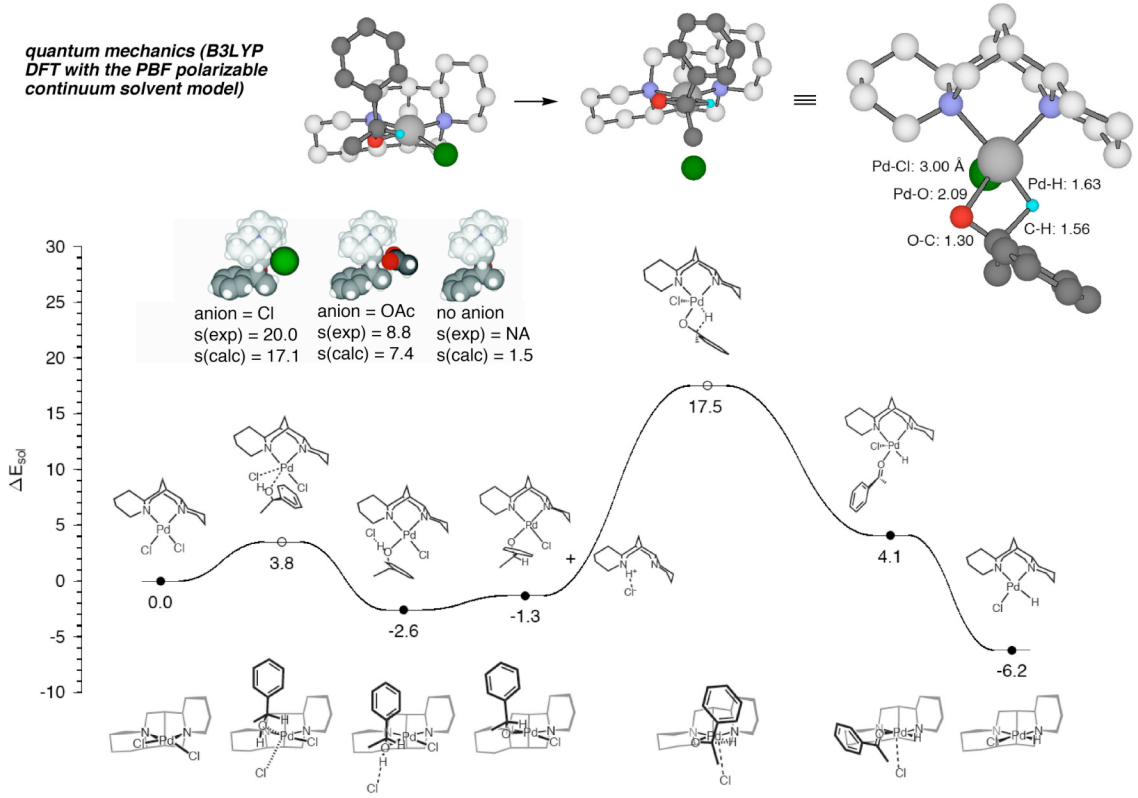

Further evidence demonstrating the key interaction between the counterion and sparteine ligand in imparting selectivity and reactivity was found in X-ray crystallographic analyses of palladium complexes relevant to the kinetic resolution. Crystallographic analysis of Pd(sparteine)Cl_2 (**66**), a catalyst precursor performing identically in the resolution to Pd(nbd)Cl_2 and 5 mol% (–)-sparteine (**28**), revealed a significant distortion in the square plane about the metal center (Figure 4.1.2).[8] The sum of the six angles around the metal center is only 705.99°, compared to 720° in an ideal square planar geometry. The majority of this deviation from planarity is due to chloride Cl2. Near the projecting N2 piperidine ring of the sterically crowded C_1 symmetric (–)-sparteine ligand, chloride Cl2 is deflected about 9.9° out of the plane of the metal

complex (180° – ∠N1–Pd–Cl2). This deformation is substantially larger than that for the less active kinetic resolution catalyst Pd(sparteine)$(OAc)_2$ (**231**, Figure 4.1.3), in which the sum of the six angles about the palladium center and acetate deflection are 711.36° and 5.4°, respectively.[9]

Figure 4.1.2 Structure of Pd(sparteine)Cl_2.

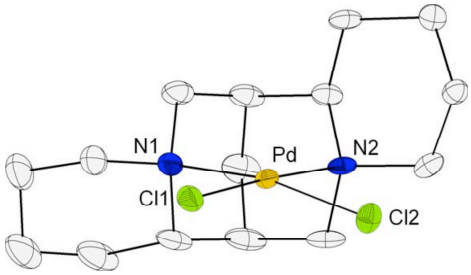

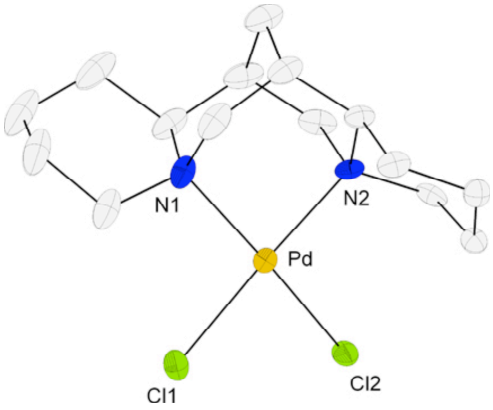

Select bond lengths (Å) and angles (°)			
Pd–N1	2.127(3)	N1–Pd–N2	87.51(10)°
Pd–N2	2.096(2)	Cl1–Pd–Cl2	83.09(3)°
Pd–Cl1	2.3161(9)	N2–Pd–Cl1	176.24(7)°
Pd–Cl2	2.3150(8)	N1–Pd–Cl2	170.06(8)°
		N1–Pd–Cl1	95.65(8)°
		N2–Pd–Cl2	93.44(7)°
		Σ ∠	705.99°

Figure 4.1.3 Structure of Pd(sparteine)$(OAc)_2$.

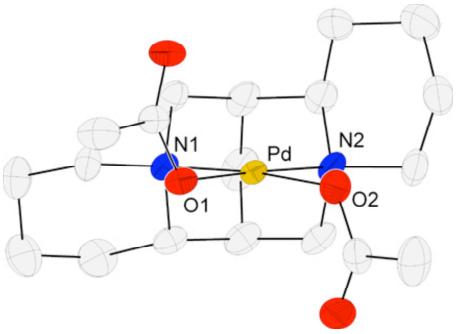

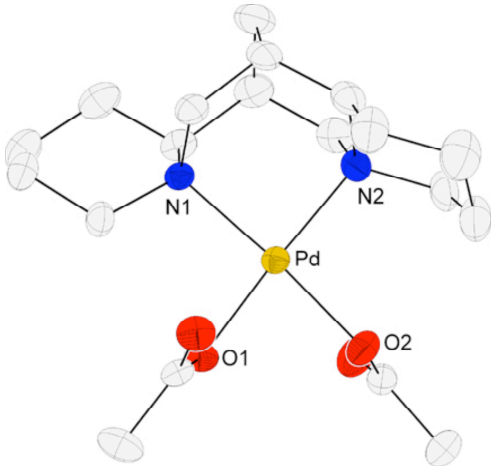

Select bond lengths (Å) and angles (°)			
Pd–N1	2.096(2)	N1–Pd–N2	88.41(8)°
Pd–N2	2.066(3)	O1–Pd–O2	82.58(9)°
Pd–O1	2.021(2)	N2–Pd–O1	176.83(10)°
Pd–O2	2.030(2)	N1–Pd–O2	174.65(9)°
		N1–Pd–O1	94.22(8)°
		N2–Pd–O2	94.67(9)°
		Σ ∠	711.36°

Raissa Trend, a graduate student in these laboratories, synthesized a number of palladium complexes to better understand the structural features and reactivity of Pd(sparteine)Cl_2 (**66**). Utilizing a trifluoromethyl derivative of (*R*)-1-phenylethanol ((+)-**25**), which is the faster reacting enantiomer in the oxidative kinetic resolution, she was able to prepare alkoxide **232** (Figure 4.1.4).[8] This complex is even more distorted from an ideal square plane than Pd(sparteine)Cl_2. The sum of the six bond angles around the metal center is 701.58°, and the chloride deflection is 15.4°. Interestingly, the benzylic C–H bond of the alkoxide aligned with the Pd-Cl bond. This orientation is expected to be similar to that required to displace the chloride ligand and form a β-agostic interaction between the benzylic C–H bond and the palladium center in the calculated transition state for β-hydride elimination. Presumably, β-hydride elimination does not occur because the electron-withdrawing trifluoromethyl group disfavors the formation of an actual β-agostic interaction in this complex.

Figure 4.1.4 Structure of palladium alkoxide **232**.

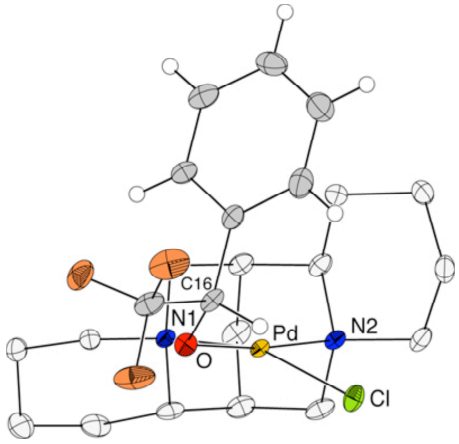

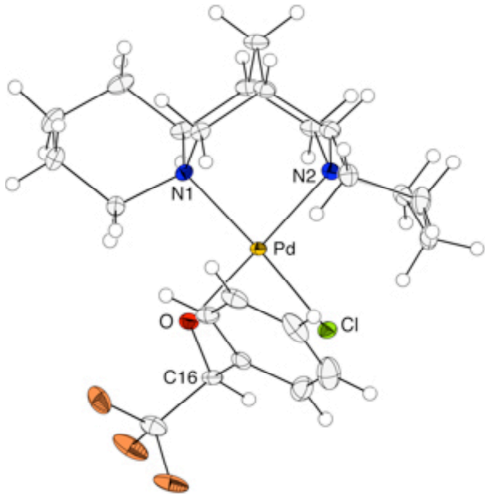

Select bond lengths (Å) and angles (°)			
Pd–N1	2.1243(17)	N1–Pd–N2	88.07(6)°
Pd–N2	2.0925(16)	O–Pd–Cl	87.71(4)°
Pd–O	2.0012(14)	N2–Pd–O	176.27(6)°
Pd–Cl	2.3316(5)	N1–Pd–Cl	164.59(5)°
		N1–Pd–O	89.78(6)°
		N2–Pd–Cl	95.16(4)°
		Σ ∠	701.58°

Based on crystallographic studies, as well as kinetic[7] and theoretical[6] work in this area, a model for reactivity and selectivity in the oxidative kinetic resolution was developed (Scheme 4.1.3, R^L = large substituent, R^S = small substituent).[8] When a racemic alcohol mixture is exposed to Pd(sparteine)Cl_2 (**66**), a diastereomeric mixture of palladium alkoxides **233** and **235** are formed. Complex **233**, formed with the faster reacting enantiomer of alcohol, proceeds through a β-hydride elimination transition state (**234**) similar to trifluoromethyl alkoxide **232**, in which the chloride counterion has been fully displaced into the apical position of the palladium complex. Subsequent β-hydride elimination leads to product ketone. Diastereomeric complex **235**, on the other hand, is unable to proceed through an intermediate similar to alkoxide **232** without destabilizing steric interactions between R^L and the chloride counterion. This unfavorable interaction

is even greater in transition state **238**. Alternatively for complex **235**, the C–H bond could approach the palladium center from the opposite side of the square plane, as in complex **237**. However, this geometry would be expected to lead to destabilizing interactions between R^L and one of the piperidine rings of the sparteine framework, as well as deflecting the chloride counterion into the other piperidine ring, which projects over the square plane of the complex. Thus, diastereomer **235** is reprotonated to form the resolved alcohol.

Scheme 4.1.3 Model for selectivity of the resolution.

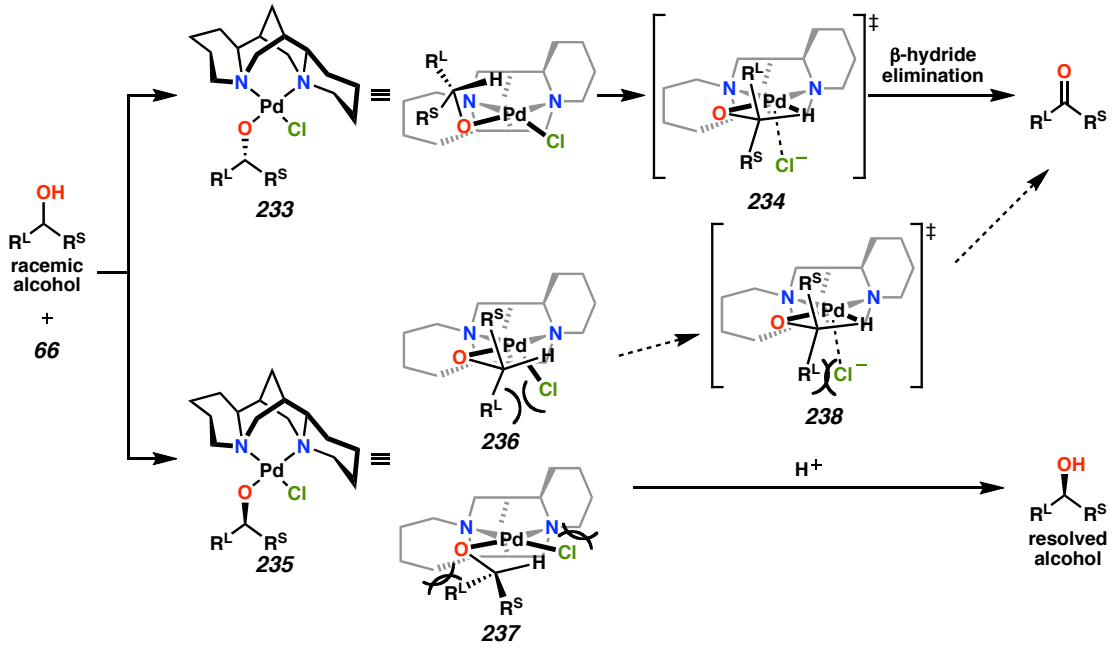

4.2 Counterion Studies in the Kinetic Resolution

4.2.1 Phenoxides

The previous computational and crystallographic studies have demonstrated the importance of the counterion for selectivity in the oxidation. However, the observed counterion distortion in a number of palladium complexes is intriguing. The greater the

counterion deflection in the complex, the more the geometry of the complex resembles that of the β-hydride elimination transition state. We reasoned that a complex with a greater counterion distortion might have a lower energy barrier to the rate-limiting β-hydride elimination, leading to increased rates of alcohol oxidation. Therefore, the interaction between the (–)-sparteine ligand and the counterion could be important for both selectivity and reactivity in the kinetic resolution. This hypothesis could explain why Pd(sparteine)Cl_2 (**66**) is both more selective and more reactive as a catalyst than Pd(sparteine)$(OAc)_2$ (**231**). Because of the critical role of counterion in the resolution, this area has been explored further to potentially provide even better catalysts for this useful transformation.

Jeffrey Bagdanoff, a graduate student in these laboratories, initiated a project utilizing salts of alcohols either resistant to β-hydride elimination or lacking β-hydrides completely as counterions in the resolution.[10] These counterions were expected to be easily modifiable, allowing for greater control of steric and electronic properties of the resulting palladium complex. Indeed, Jeffrey Bagdanoff was able to prepare and crystallize Pd(sparteine)$(OC_6F_5)_2$ (**239**) by simply stirring dichloride complex **66** with two equivalents of the sodium salt of pentafluorophenol (Figure 4.2.1). This complex exhibits a distorted square planar geometry, with the sum of the six bond angles around the palladium center and N1–Pd–O2 deflection of 710.98° and 7.5°, respectively. Based on our hypothesis, the bond angles observed suggested that this palladium complex would be less active in the oxidative kinetic resolution than Pd(sparteine)Cl_2 (**66**).

Figure 4.2.1 Structure of Pd(sparteine)(OC_6F_5)$_2$.

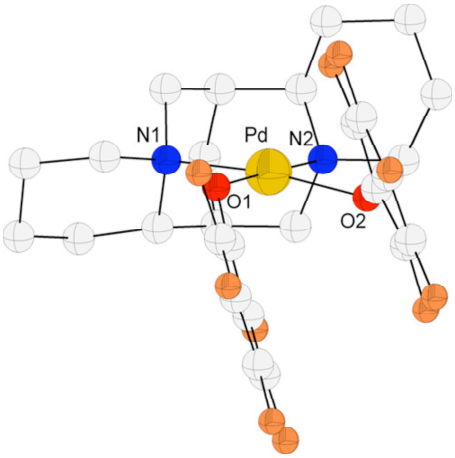

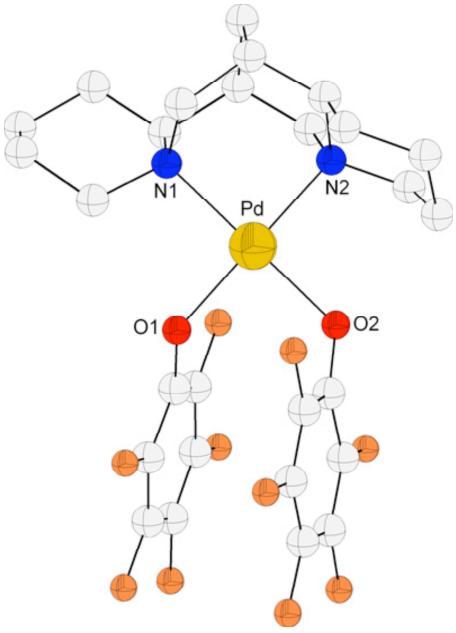

Select bond lengths (Å) and angles (°)			
Pd–N1	2.114(5)	N1–Pd–N2	88.5(2)°
Pd–N2	2.067(5)	O1–Pd–O2	88.96(16)°
Pd–O1	2.024(4)	N2–Pd–O1	178.6(2)°
Pd–O2	2.034(5)	N1–Pd–O2	172.50(19)°
		N1–Pd–O1	91.72(18)°
		N2–Pd–O2	90.7(2)°
		Σ ∠	710.98°

When generated in situ, Jeffrey Bagdanoff found that complex **239** was a poor catalyst for the enantioselective aerobic oxidation of (±)-1-phenylpropanol ((±)-**83**) (entry 3, Table 4.2.1). Indeed, use of the sodium salt of trifluoroethanol as the counterion also led to little oxidation (entry 2). Modest reactivity and selectivity was observed with sodium phenoxide (entry 4), although the control reaction without alkoxide was better (entry 1). Electron-rich phenoxides, however, provided much more promising results. Increased oxidation rates and selectivity were observed, leading to high enantiomeric excess of alcohol (–)-**83** (entries 5 and 6).

Table 4.2.1 Phenoxide screen with (±)-1-phenylpropanol.

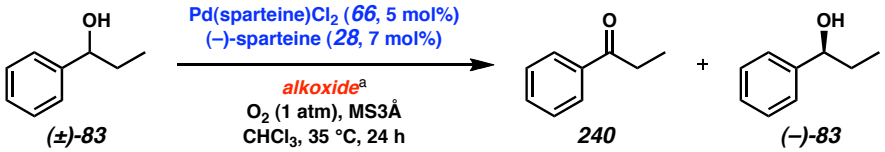

entry	alkoxide[b]	conversion[c]	alcohol ee[d]	*s*
1	none	36.5%	53.1%	27
2	$NaOCH_2CF_3$	1.2%	0.0%	–
3	$NaOC_6F_5$	3.1%	1.8%	3.6
4	NaOPh	22.8%	25.1%	16
5	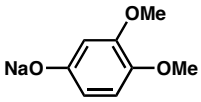	56.4%	97.3%	30
6	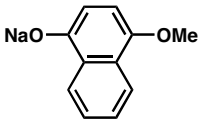	48.2%	83.6%	49

[a] Pd(sparteine)Cl_2 (**66**), (–)-sparteine (**28**), and alkoxide were sonicated in $CHCl_3$ 1 h prior to addition of (±)-**83**. [b] Prepared by treatment of the corresponding alcohol with Na (1 equiv) in toluene followed by concentration under reduced pressure. [c] Measured by GC. [d] Measured by chiral HPLC.

Further efforts in this area sought to build upon Jeffrey Bagdanoff's results with electron-rich phenoxides. Many of the corresponding phenols are commercially available. Furthermore, the sodium alkoxides are readily prepared by treatment of the phenol with metallic sodium in toluene, so a large number of phenoxides can be screened quickly. Generally, the more electron-rich phenoxides provide higher oxidation rates in the kinetic resolution of alcohol (±)-**25** (Table 4.2.2, entries 3-5) as compared to the previously reported conditions with cesium carbonate (entry 1).[11] Phenoxides with ortho substituents produce less active catalyst systems (entry 7), though these reactions still proceed to high alcohol enantiomeric excesses at prolonged reaction times. Addition of naphthoxides can lead to faster oxidation rates (entries 8 and 9) or slower rates with somewhat higher selectivity (entry 10).

Table 4.2.2 Phenoxide screen with (±)-1-phenylethanol.

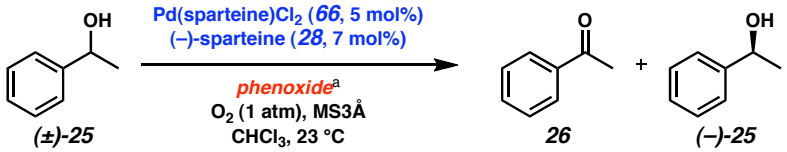

entry	phenoxide[b]	time	conversion[c]	alcohol ee[d]	*s*
1[e]	none	24 h	58.3%	97.8%	24
2	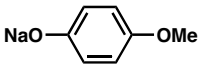	24 h	50.4%	85.7%	32
3	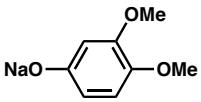	16 h	55.4%	94.0%	25
4	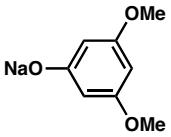	16 h	51.6%	87.6%	29
5	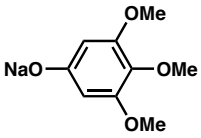	16 h	60.0%	99.5%	28
6	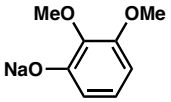	24 h	54.6%	93.5%	27
7	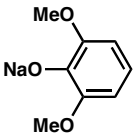	98 h	62.5%	98.1%	17
8	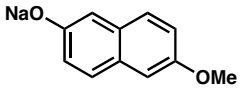	24 h	66.7%	>99.5%	>15
9	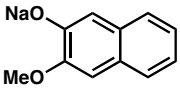	16 h	55.5%	95.0%	27
10	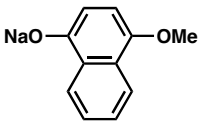	24 h	42.2%	64.8%	32

[a] Pd(sparteine)Cl_2 (**66**), (–)-sparteine (**28**), and alkoxide were stirred in $CHCl_3$ 1 h prior to addition of (±)-**25**. [b] Prepared by treatment of the corresponding phenol with Na (1 equiv) in toluene followed by concentration under reduced pressure. [c] Measured by GC. [d] Measured by chiral HPLC. [e] Cs_2CO_3 (40 mol%) was added.

While (±)-1-phenylethanol ((±)-**25**) was able to be resolved with a number of added phenoxides, a more challenging substrate for the enantioselective oxidation was sought in order to highlight the beneficial role of these additives. Alcohol (±)-**73** was a problematic substrate for the previously developed conditions, generally being resolved only at extended reaction times and with modest selectivity. Thus, phenoxides were explored in order to improve this resolution (Table 4.2.3). Many of the previously investigated phenoxides (entries 2-4, 6-8, 13, 14, and 18) lead to results that are not substantially different than those with cesium carbonate (entry 1). A number of other phenoxides (entries 5, 9-11, and 15) provide decreased oxidation rates. However, several naphthoxides (entries 12, 16, and 17) result in promising improvements in the selectivity of the kinetic resolution of this alcohol.

Table 4.2.3 Phenoxide screen with secondary alcohol (±)-**73**.

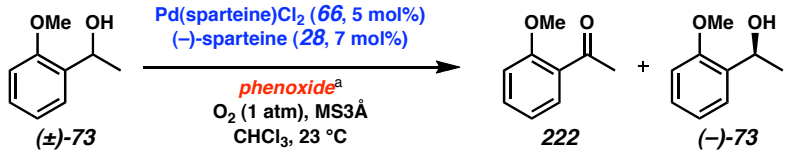

entry	phenoxide[b]	time	conversion[c]	alcohol ee[d]	*s*
1[e]	none	46 h	48.3%	66.0%	11
2	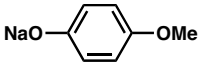	46 h	42.7%	52.3%	9.5
3	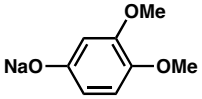	46 h	55.6%	82.6%	12
4		114 h	69.8%	99.1%	12
5	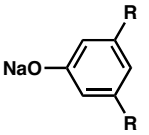 R = Me	114 h	45.2%	54.8%	8.5
6	R = OMe	46 h	50.4%	72.3%	13
7	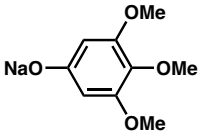	46 h	46.8%	63.6%	12
8	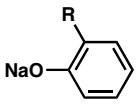 R = Me	46 h	48.8%	65.7%	11
9	R = Cl	118 h	39.3%	49.3%	12
10	R = OMe	118 h	46.8%	61.9%	11
11	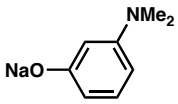	118 h	62.1%	92.8%	12
12	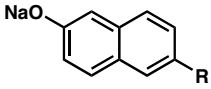 R = H	62 h	56.8%	88.8%	15
13	R = OMe	46 h	46.9%	65.1%	13
14	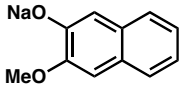	46 h	42.6%	56.7%	13
15	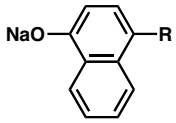 R = H	115 h	49.8%	67.8%	11
16	R = Cl	115 h	36.7%	50.2%	23
17	R = OMe	114 h	47.5%	73.9%	22
18	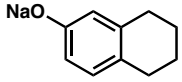	46 h	45.7%	58.6%	10

[a] Pd(sparteine)Cl_2 (**66**), (–)-sparteine (**28**), and alkoxide were stirred in $CHCl_3$ 1 h prior to addition of (±)-**73**. [b] Prepared by treatment of the corresponding phenol with Na (1 equiv) in toluene followed by concentration under reduced pressure. [c] Measured by GC. [d] Measured by chiral HPLC. [e] Cs_2CO_3 (40 mol%) was added.

The similar results for a wide range of phenoxides as additives in the kinetic resolution imply that instead of forming a discrete palladium phenoxide complex, the electron-rich phenoxides could just be acting as soluble bases. Some evidence indicating that palladium phenoxides are forming in situ include the isolation and crystallographic analysis of Pd(sparteine)(OC_6F_5)$_2$ (**239**) and the impact of steric effects on the rates of oxidation with some phenoxides (Table 4.2.3, entries 9, 10, and 15-17). Unfortunately, the isolation of palladium complexes with more electron-rich phenoxides that are active precatalysts in the oxidative kinetic resolution has been unsuccessful to date.

For further studies, two enantiomeric BINOL-derived phenoxides were prepared[12] and used as additives in the kinetic resolution (Table 4.2.4). While there is a difference in the initial oxidation rates of the resolutions, the outcomes of the resolutions are nearly identical, with selectivity factors of 20-21 in both cases. Either no palladium phenoxide complexes are formed in these reactions and the phenoxides are acting as soluble non-enantioselective bases, or the enantiomeric BINOL-derived phenoxides impart no chiral influence on the reaction when the two diastereomeric palladium phenoxide complexes are formed in situ.

Table 4.2.4 BINOL-derived phenoxides as additives.

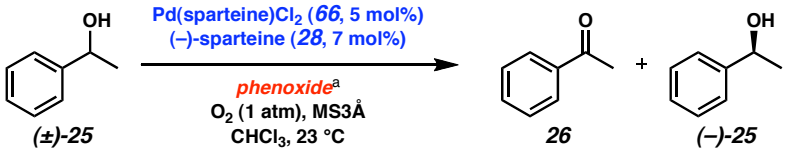

entry	phenoxide[b]	time	conversion[c]	alcohol ee[d]	*s*
1	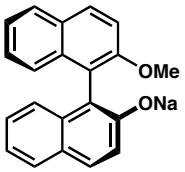	19 h	37.7%	51.3%	20
2		43 h	62.7%	>99%	>21
3	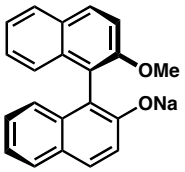	19 h	50.4%	80.4%	21
4		43 h	61.4%	>99%	>21

[a] Pd(sparteine)Cl_2 (**66**), (–)-sparteine (**28**), and alkoxide were stirred in $CHCl_3$ 1 h prior to addition of (±)-**25**. [b] Prepared by treatment of the corresponding phenol with Na (1 equiv) in toluene followed by concentration under reduced pressure. [c] Measured by GC. [d] Measured by chiral HPLC.

If a palladium bis-phenoxide complex is forming in situ, then the catalyst precursor should have little influence on the outcome of the resolution. To test this hypothesis, the sodium salt of 6-methoxy-2-naphthol was added to resolutions with a number of palladium precursors (Table 4.2.5). As described previously, reaction rate and selectivity are similar with Pd(sparteine)Cl_2 (**66**) and cesium carbonate or the naphthoxide (entries 1 and 2). However, in the case of Pd(sparteine)$(OAc)_2$ (**231**) or Pd(sparteine)$(TFA)_2$ (**241**),[13] which both display decreased selectivity with cesium carbonate (entries 3 and 5, respectively), a substantial improvement in the *s* factors is observed on addition of naphthoxide (entries 4 and 6). While the catalysts in these systems are still not as active as in the case of dichloride complex **66**, these results still demonstrate that phenoxides can have a large impact on the selectivity of the kinetic resolution. Because the selectivity is dictated by β-hydride elimination from a palladium

alkoxide complex, these results present strong evidence for the formation of palladium phenoxide complexes in situ.

Table 4.2.5 Counterion variation with phenoxides.

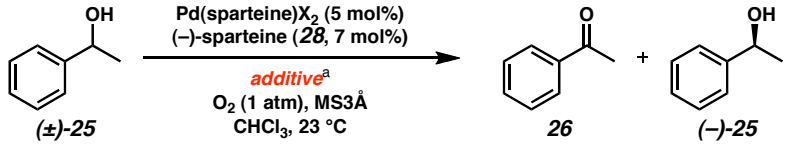

entry	X	additive[b]	time	conversion[c]	alcohol ee[d]	*s*
1	Cl	Cs_2CO_3 (40 mol%)	24 h	58.3%	97.8%	24
2	Cl	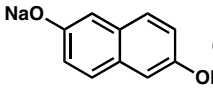 (10 mol%)	24 h	56.7%	97.6%	30
3	OAc	Cs_2CO_3 (40 mol%)	48 h	54.4%	72.8%	8.8
4	OAc	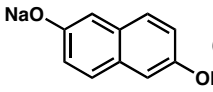 (10 mol%)	48 h	35.8%	50.2%	31
5	TFA	Cs_2CO_3 (40 mol%)	48 h	60.4%	85.0%	9.1
6	TFA	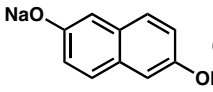 (10 mol%)	48 h	59.4%	95.0%	17

[a] Pd(sparteine)X_2, (–)-sparteine (**28**), and alkoxide were stirred in $CHCl_3$ 1 h prior to addition of (±)-**25**. [b] Phenoxide prepared by treatment of the phenol with Na (1 equiv) in toluene followed by concentration under reduced pressure. [c] Measured by GC. [d] Measured by chiral HPLC.

4.2.2 Bromide as Counterion in the Resolution

While phenoxides show promise in the oxidative kinetic resolution, other counterions have also been explored. Eric Ferreira had previously shown that $PdBr_2$ was not a good catalyst for alcohol oxidation at 80 °C (Table 4.1.1). The reaction rapidly darkened, indicating the aggregation of palladium(0). However, a crystal structure of Pd(sparteine)Br_2 (**242**) obtained by Raissa Trend led to a reinvestigation of bromide as a counterion.[1,14] As shown in Figure 4.2.2, the square plane of this complex is quite distorted. The sum of the six bond angles around the palladium center is 699.22°, largely

due to the 14.0° deflection of Br2 out of the plane. This much larger counterion distortion suggests that dibromide complex **242** could be a more active catalyst for the oxidative kinetic resolution than dichloride complex **66**.

Figure 4.2.2 Structure of Pd(sparteine)Br_2.

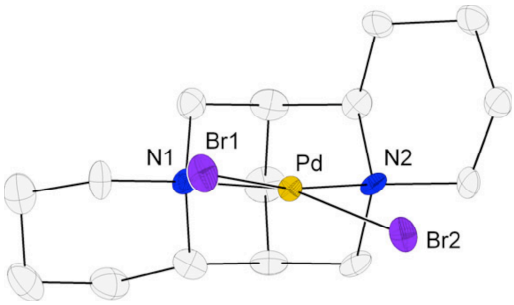

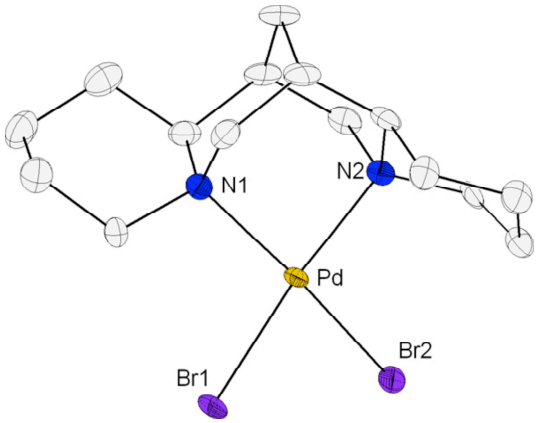

Select bond lengths (Å) and angles (°)			
Pd–N1	2.1510(18)	N1–Pd–N2	87.43(7)°
Pd–N2	2.1184(16)	Br1–Pd–Br2	84.155(10)°
Pd–Br1	2.4560(3)	N2–Pd–Br1	171.20(5)°
Pd–Br2	2.4474(3)	N1–Pd–Br2	165.96(5)°
		N1–Pd–Br1	96.25(5)°
		N2–Pd–Br2	94.22(5)°
		Σ ∠	699.22°

To more easily distinguish between the oxidation rates and selectivities of various catalysts, oxidations with the faster reacting enantiomer of 1-phenylethanol ((+)-**25**) were conducted (Table 4.2.6). In reactions conducted in chloroform at 23 °C, Pd(sparteine)Br_2 (**242**, entry 2) displays the highest reactivity, achieving 72.0% conversion to acetophenone (**26**) in only 4 h. Pd(sparteine)Cl_2 (**66**, entry 1) is significantly less active, providing 38.9% conversion. Several other palladium complexes (entries 3-5) have even lower rates of oxidation.

Table 4.2.6 Rate of oxidation of various palladium precatalysts.

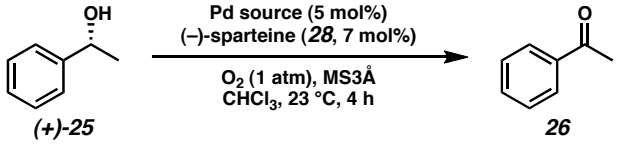

entry	Pd source	conversion[a]
1	Pd(sparteine)Cl_2 (***66***)	38.9%
2	Pd(sparteine)Br_2 (***242***)	72.0%
3	Pd(sparteine)I_2 (***243***)	17.5%
4	Pd(sparteine)$(OAc)_2$ (***231***)	7.8%
5	Pd(sparteine)$(TFA)_2$ (***241***)	30.3%

[a] Measured by GC.

In situ generation of the active catalyst with a number of palladium bromide sources and 12 mol% (–)-sparteine (**28**) was investigated (Table 4.2.7). $PdBr_2$ leads to a slower rate of oxidation (entry 1). The lower solubility of $PdBr_2$ may result in incomplete formation of Pd(sparteine)Br_2 in situ and therefore less of the active catalyst in solution. On the other hand, more soluble palladium bromide sources (entries 2-4) are viable as catalyst precursors and provide similar rates and only slightly decreased selectivity relative to the preformed complex (entry 5).

Table 4.2.7 Various dibromide precursors in the resolution.

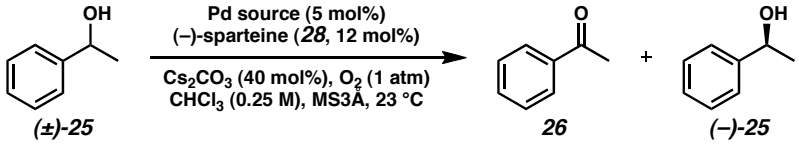

entry	Pd source	time	conversion[a]	alcohol ee[b]	*s*
1	$PdBr_2$	24 h	52.1%	88.1%	27
2	Pd$(CH_3CN)_2Br_2$ (***244***)	4.5 h	59.0%	97.6%	22
3	Pd(COD)Br_2 (***245***)	4.5 h	59.0%	97.3%	21
4	Pd(nbd)Br_2 (***246***)	4.5 h	48.2%	76.4%	23
5[c]	Pd(sparteine)Br_2 (***242***)	4 h	55.6%	95.6%	28

[a] Measured by GC. [b] Measured by chiral HPLC. [c] 7 mol% (–)-sparteine (**28**) added.

The optimal solvent for reactions with Pd(sparteine)Cl_2 (**66**) was chloroform,[11] so this solvent was chosen for the previous screens. However, a more thorough solvent investigation was undertaken at 23 °C (Table 4.2.8). Chlorinated solvents lead to the most rapid oxidations (entries 1-3). Dichloromethane has proven to be an even better solvent for high reaction rates. However, selectivity is decreased slightly with this solvent. Reactions in both acetone and 2-butanone (entries 5 and 6) display reasonable reaction rates and maintain the selectivity of reactions conducted in chloroform. Resolutions in tetrahydrofuran, *tert*-butyl alcohol, *p*-dioxane, and ethyl acetate (entries 9-12) exhibit excellent selectivity, but at the cost of prohibitively long reaction times. Toluene, a solvent successfully used previously in conditions with Pd(sparteine)Cl_2 (**66**), also performs well with Pd(sparteine)Br_2 (**242**). Though much slower than in chlorinated solvents or in acetone, oxidations are highly selective in toluene. Interestingly, *N*,*N*-dimethylformamide and acetonitrile (entries 4 and 7) support oxidations at comparable rates to acetone, but with substantially decreased selectivity. By and large, *s* factors are higher for solvents with lower dielectric constants. The more polar solvents could stabilize a larger counterion separation in the β-hydride elimination transition state, resulting in the observed decreased selectivity. The general trends in reactivity are harder to understand. Dielectric constants do not seem to account for the differences.[15] Catalyst solubility could be an important factor, as Pd(sparteine)Br_2 (**242**) is poorly soluble in most non-chlorinated solvents.

Table 4.2.8 Solvent screen with Pd(sparteine)Br_2.

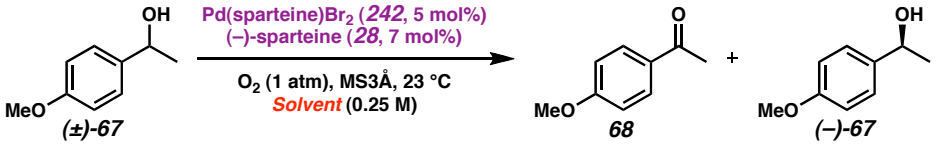

entry	solvent	dielectric constant	time	conversion[a]	alcohol ee[b]	*s*
1	CH_2Cl_2	8.93	2 h	61.5%	96.4%	15
2	DCE	10.42	4 h	56.6%	90.9%	17
3	***$CHCl_3$***	***4.81***	***4 h***	***55.2%***	***91.9%***	***22***
4	DMF	38.25	20 h	57.7%	73.0%	6.9
5	***acetone***	***21.01***	***30 h***	***55.9%***	***94.1%***	***23***
6	2-butanone	18.56	30 h	55.2%	91.6%	21
7	CH_3CN	36.64	30 h	54.7%	75.9%	10
8	***$PhCH_3$***	***2.38***	***50 h***	***52.1%***	***92.5%***	***41***
9	THF	7.52	144 h	54.8%	97.8%	41
10	*t*-BuOH	12.47	195 h	55.2%	96.8%	34
11	*p*-dioxane	2.22	120 h	38.1%	59.3%	98
12	EtOAc	6.08	144 h	39.3%	61.6%	76
13	H_2O:acetone (1:1)	80.10/21.01	72 h	19.8%	20.4%	13
14	$MeNO_2$	37.27	120 h	10.6%	–	–
15	pinacolone	12.73	48 h	2.8%	–	–
16	MTBE	–	48 h	1.3%	–	–

[a] Measured by GC. [b] Measured by chiral HPLC.

Optimization of conditions in toluene led to a number of useful resolution conditions (Table 4.2.9). Added cesium carbonate has a beneficial effect on oxidation rate in most resolutions with Pd(sparteine)Br_2 (**242**) in toluene (entries 3-5), as is the case with Pd(sparteine)Cl_2 (**66**) as catalyst. However, this exogenous base is slightly detrimental to the rate and selectivity of resolutions with dibromide complex **242** conducted at 23 °C (cf. entries 1 and 2). Presumably, the initial rate increase with added exogenous base is offset by formation of Pd(sparteine)(CO_3) (**69**), previously shown to be an inactive palladium complex generated under kinetic resolution conditions with

Pd(sparteine)Cl_2 (**66**).[16] Kinetic resolutions with dibromide complex **242** conducted at 60 °C under an atmosphere of molecular oxygen have exceptional rates (entry 3). As seen previously by Eric Ferreira (Table 4.1.1, entry 5), reactions conducted above 60 °C with Pd(sparteine)Br_2 (**242**) rapidly lose catalytic activity and become black, indicating palladium(0) aggregation. This system is also viable under ambient air atmosphere (entries 4 and 5). However, resolutions under ambient air in toluene must be conducted below 60 °C to prevent catalyst decomposition.

Table 4.2.9 Pd(sparteine)Br_2 conditions in toluene.

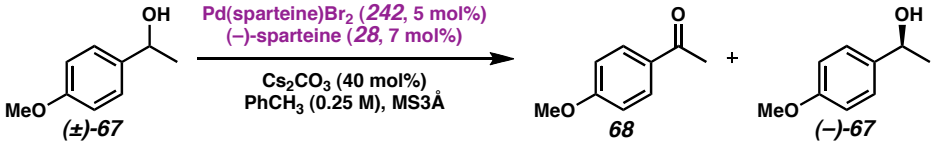

entry	temperature	oxidant (1 atm)	time	conversion[a]	alcohol ee[b]	*s*
1[c]	23 °C	O_2	50 h	52.1%	92.5%	41
2	23 °C	O_2	72 h	52.9%	88.6%	25
3	60 °C	O_2	3 h	52.4%	92.7%	39
4[d]	50 °C	air	4.5 h	57.0%	96.9%	26
5[d]	23 °C	air	50 h	54.8%	98.3%	44

[a] Measured by GC. [b] Measured by chiral HPLC. [c] No Cs_2CO_3. [d] Conducted with 15 mol% (–)-sparteine (**28**).

Conditions with Pd(sparteine)Br_2 (**242**) as catalyst in either toluene at 60 °C or chloroform at 23 °C are much more active in the oxidation of secondary alcohols than similar conditions with Pd(sparteine)Cl_2 (**66**). Thus, we looked to apply these more reactive systems to the kinetic resolution of alcohols that had proven challenging for our previous systems.[17] Table 4.2.10 displays a variety of secondary alcohols that require prolonged reaction times to reach even modest enantiomeric excesses. Several hindered benzylic alcohols (entries 1-3), enol ether **98** (entry 4), and non-activated alkyl alcohol

136 (entry 5) are slow to oxidize under conditions with Pd(sparteine)Cl_2 (**66**) in chloroform.

Table 4.2.10 Slow substrates with Pd(sparteine)Cl_2.

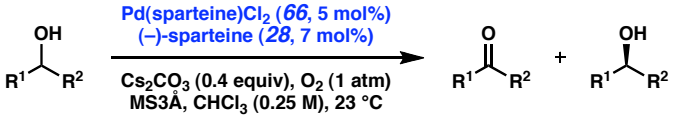

entry	alcohol, major enantiomer	time	conversion[a]	alcohol ee[b]	*s*
1	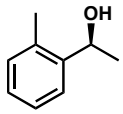 ***(–)-72***	63 h	40.1%	49.2%	11
2	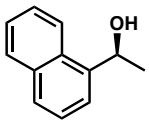 ***(–)-78***	97 h	51.2%	65.9%	8.5
3	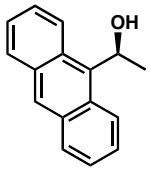 ***(–)-247***	48 h	21.8%	– [c]	–
4	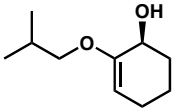 ***(S)-98***	74 h	52.2%	85.9%	23
5	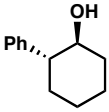 ***(+)-136***	93 h	38.2%	46.9%	12

[a] Measured by GC. [b] Measured by chiral HPLC. [c] Not determined.

When these alcohols are exposed to conditions with Pd(sparteine)Br_2 (**242**) in chloroform, on the other hand, successful resolutions are achieved (Table 4.2.11). Hindered benzylic alcohols (entries 6-10) are able to be resolved in reasonable times with increased selectivity relative to conditions with dichloride complex **66**. Even alkyl alcohol **136** (entries 12 and 13), which lacks an adjacent activating group such as an aromatic ring or alkene, can be resolved to high enantiomeric excess. Substrates that are

successfully resolved with Pd(sparteine)Cl_2 (**66**) can also be selectively oxidized with Pd(sparteine)Br_2 (**242**) (entries 1-5), but with substantially shorter reaction times. This catalyst system is sufficiently active to perform oxidations at temperatures below 23 °C too (entries 4 and 5). Finally, ambient air is competent as the terminal oxidant in these resolutions (entries 2, 7, 9, and 13), providing comparable rates and selectivities to reactions conducted under an atmosphere of molecular oxygen (entries 1, 6, 8, and 12).

Table 4.2.11 Substrate scope with Pd(sparteine)Br_2.

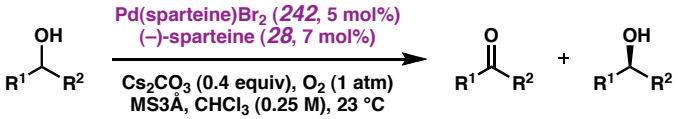

entry	alcohol, major enantiomer	time	conversion[a] (yield)[b]	alcohol ee[c]	*s*
1	 *(–)-25*	4 h	55.6% (43%)	95.6%	28
2[d]		5 h	55.3%	94.7%	27
3	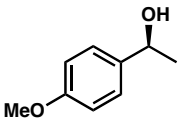 *(–)-67*	4 h	59.4% (41%)	95.4%	17
4[e]		8 h	59.3%	96.9%	20
5[f]	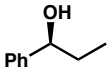 *(–)-83*	24 h	59.9%	97.8%	20
6	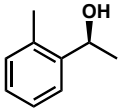 *(–)-72*	41 h	63.5% (35%)	97.1%	14
7[d]		30 h	63.4%	96.2%	13
8	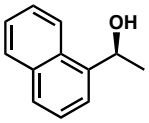 *(–)-78*	24 h	59.6% (40%)	92.5%	14
9[d]		21 h	64.9%	98.5%	15
10	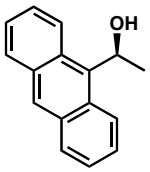 *(–)-247*	15 h	60.0%	91.2%	12
11	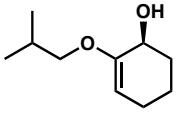 *(S)-98*	48 h	61.6%	97.0%	16
12	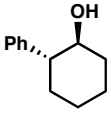 *(+)-136*	49 h	58.0% (40%)	90.6%	15
13[d]		45 h	57.7%	91.0%	15

[a] Measured by GC or ^{1}H NMR. [b] Isolated yield of enantioenriched alcohol. [c] Measured by chiral HPLC or GC. [d] Performed under ambient air. [e] Performed at 10 °C. [f] Performed at 4 °C.

4.3 Neutral Ligand Studies

4.3.1 Background and Early Results

In addition to exploring the counterion ligand for the palladium catalyst, we have also investigated the neutral ligand in the oxidative kinetic resolution. (–)-Sparteine (**28**)

emerged as the sole successful ligand in early studies by Eric Ferreira.[3] While the commercial availability of this diamine made it an attractive ligand for this process, the scarcity of its enantiomer (*ent*-(+)-**28**) was a major limitation to the broad utility of the method.[18] Thus, we sought an alternative chiral ligand for the resolution.[19]

Eric Ferreira and Jeffrey Bagdanoff explored a large number of potential ligands for the oxidative kinetic resolution (Figure 4.3.1). A range of bisoxazolines, bispidines, diamines, monoamines, and phosphines were examined. None of these compounds promoted significant enantioselective oxidation of secondary alcohols.[10]

Figure 4.3.1 Previously examined unsuccessful ligands.

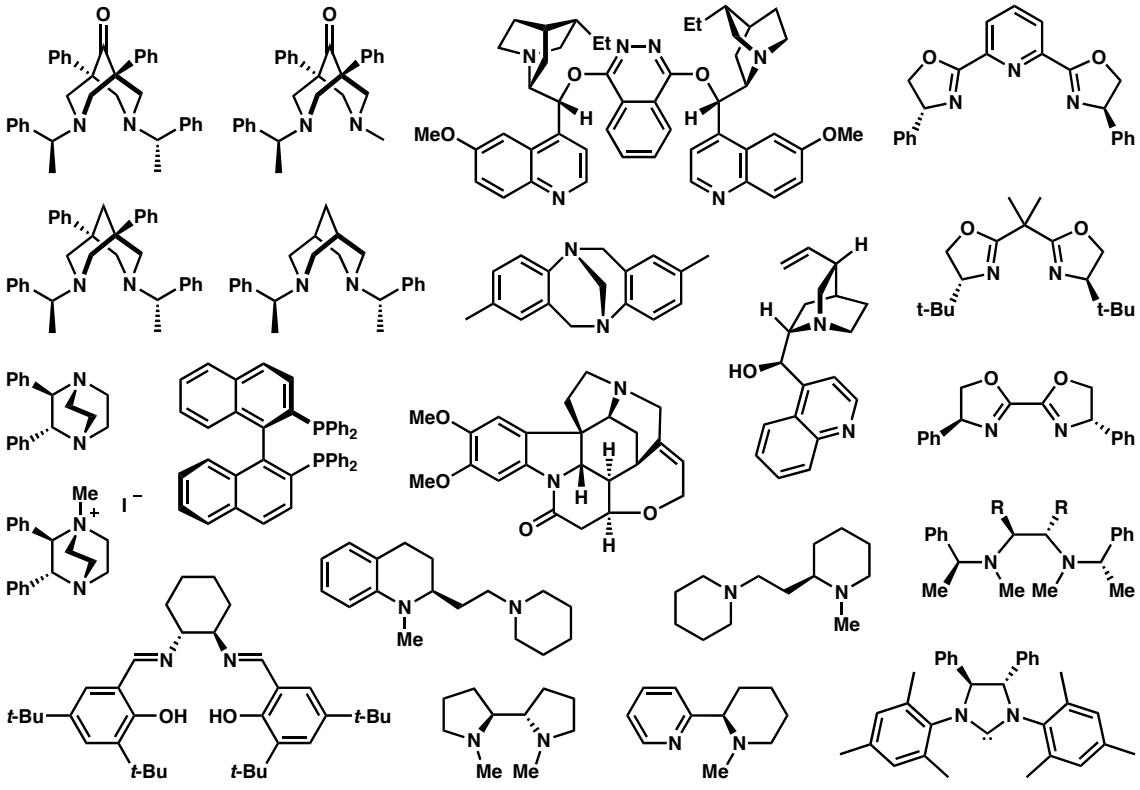

Our efforts built upon the lessons learned in these early experiments. Many common ligands, such as electron-rich phosphines, are unstable to the aerobic conditions

of the resolution. However, the system requires a sufficiently electron-rich ligand to strongly coordinate to the palladium center, promote enantioselective oxidation, and suppress palladium(0) aggregation. Monodentate ligands were anticipated to be too labile and unable to impart enough of a chiral influence on the kinetic resolution to be successful ligands.[20] Thus, diamines were targeted as oxidatively stable, bidentate ligands for the resolution. As seen in Figure 4.3.2, a variety of diamine motifs were investigated with $Pd(nbd)Cl_2$. Not only was there no kinetic resolution under aerobic conditions with any of the diamines, little non-enantioselective oxidation of secondary alcohols was observed.

Figure 4.3.2 Ligands not promoting oxidative kinetic resolution.

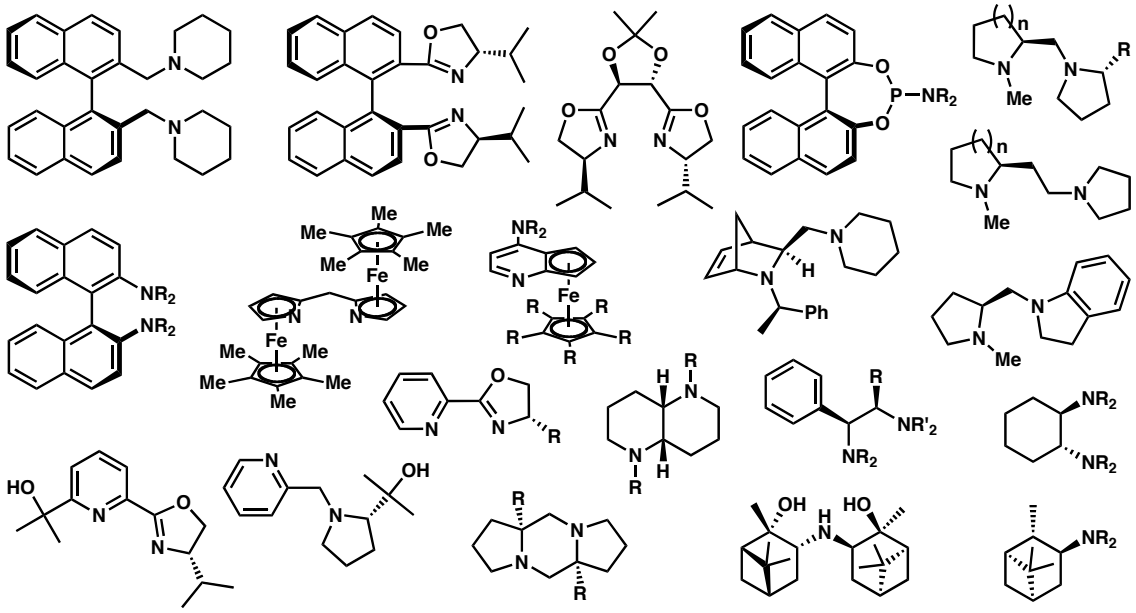

Inspiration for additional research was taken from rate studies performed by Jeffrey Bagdanoff (Table 4.3.1).[10] He evaluated a variety of diamines in the oxidation of (+)-1-phenylethanol ((+)-**25**). (–)-Sparteine (**28**) was a superior ligand for this reaction (entry 1). A number of linear diamines were largely ineffective (entries 2-4), as were

aromatic diamines (entries 7 and 8). Notably, only a diamine with a bispidine core similar to (–)-sparteine (**28**) promoted substantial alcohol oxidation (entry 9).

Table 4.3.1 Oxidation rates with various diamines.

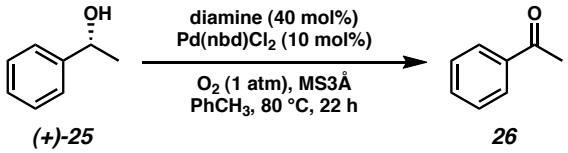

(+)-25 *26*

entry	diamine	conversion[a]	entry	diamine	conversion[a]
1	(–)-sparteine (***28***)	94.2%	6	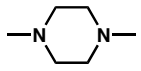	2.6%
2	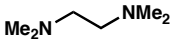	0.7%	7	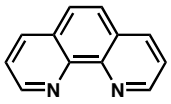	2.2%
3		8.8%			
4	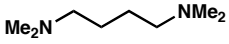	3.8%	8	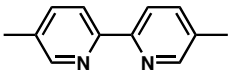	1.5%
5	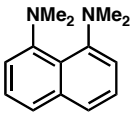	3.0%	9	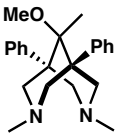	48.2%

[a] Measured by GC.

The successful oxidation with a bispidine led us to diamine **248**. O'Brien has demonstrated the ability of this diamine to act as a (+)-sparteine mimic in a number of processes (Scheme 4.3.1).[21] The enantioselective deprotonation of Boc-pyrrolidine (**249**) was accomplished by treatment with *sec*-butyllithium and diamine **248**. Subsequent trapping with chlorotrimethylsilane afforded silylpyrrolidine **250** in 90% ee.[22] The enantioselective deprotonation of cyclooctene oxide (**251**) provided alcohol **252** in 70% yield and a modest 62% ee. Finally, the deracemization of (±)-BINOL ((±)-**253**) was accomplished utilizing diamine **248** as a chiral promoter. Coordination of the diamine to copper(I) chloride, oxidation to a copper(II) species, coordination of diol (±)-**253**, thermal

equilibration, and treatment with concentrated hydrochloric acid liberated enantioenriched (+)-BINOL ((+)-**253**) in good yield and excellent enantiomeric excess.[21]

Scheme 4.3.1 Diamine **248** in asymmetric transformations.

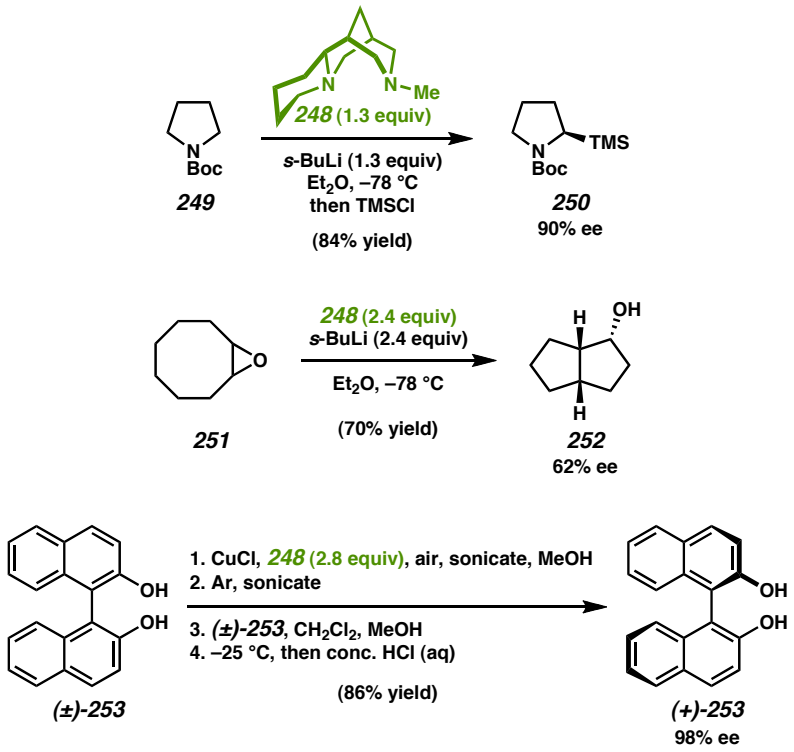

4.3.2 (–)-Cytisine-Based Diamines in the Oxidative Kinetic Resolution with $PdCl_2$

We anticipated that this diamine framework would be excellent for the kinetic resolution. Diamine **248** contains two coordinating, electron-rich tertiary amines that are stable to oxidation. Furthermore, as in the case of (–)-sparteine (**28**), this diamine contains a rigid bispidine core, which could provide a good chiral framework when coordinated to the palladium center.

A variety of potential ligands related to diamine **248** are readily prepared from (–)-cytisine (**254**). Substantial quantities of this alkaloid can be extracted from the seeds of the common decorative tree *Laburnum anagyroides*, the Golden Chain Tree.[23] From

this alkaloid, a number of known procedures can be followed to prepare diamines with a range of *N*-substitution. Acylation of the secondary amine of alkaloid **254** generates a number of amides in good to excellent yields (Scheme 4.3.2). Pyridone reduction with Adams' catalyst followed by exhaustive reduction with lithium aluminum hydride affords diamines **248** and **260**-**263**, with a variety of alkyl substituents.[23,24] Alternatively, reductive amination of (–)-cytisine (**254**) with acetone provides pyridone **264** in 95% yield. Two-step reduction yields diamine **265**.[25]

Scheme 4.3.2 Known syntheses of (–)-cytisine-based diamines.

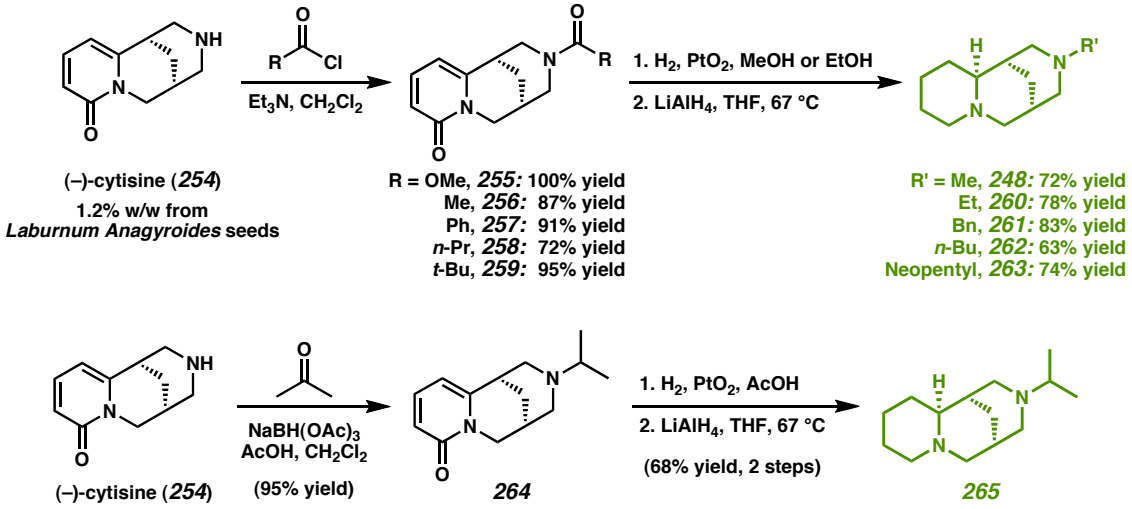

We also prepared several novel diamines (Scheme 4.3.3). Alkylation of (–)-cytisine (**254**) with isobutene oxide produces tertiary alcohol **266**.[26] Exhaustive reduction with hydrogen over Adams' catalyst and lithium aluminum hydride provides diamine **267**. Finally, hydrogenolysis of benzyl diamine **261** affords secondary amine **268**.

Scheme 4.3.3 Syntheses of novel diamines.

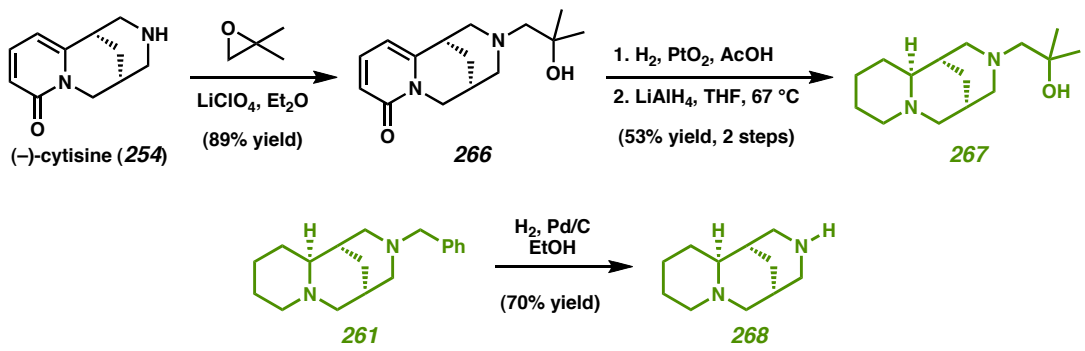

In order to assess the coordination of this structural framework to palladium salts, diamines **248** and **260** were exposed to Pd(nbd)Cl_2. Ligand exchange produces palladium complexes **269** and **270** in 83% and quantitative yields, respectively.

Scheme 4.3.4 Synthesis of dichloride complexes of diamines.

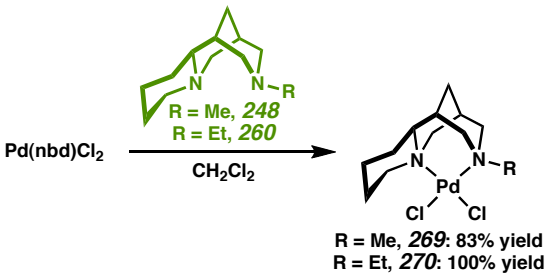

These metal complexes are readily crystallized by slow diffusion of heptane into a saturated chloroform solution. Subsequent X-ray crystallographic analysis confirms the structure of these dichloride complexes. The *N*-methyl derivative (**269**) is shown in Figure 4.3.3. This complex, like palladium complexes with (–)-sparteine (**28**), has a distorted square planar geometry, and the sum of the six bond angles around the palladium center is 704.67°. While (–)-sparteine complexes display a decreased N1–Pd–Cl2 angle, the projecting N1 piperidine ring of pseudo-enantiomeric diamine **248** results in a deflection of Cl1 of 11.9°. Because of the distortion of Cl1 instead of Cl2, we

predicted that this complex would have the opposite selectivity in the kinetic resolution, providing alcohols in the other enantiomeric series to those generated with (–)-sparteine (**28**).

Figure 4.3.3 Structure of *N*-methyl complex **269**.

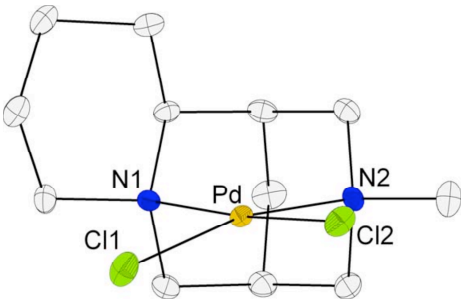

Select bond lengths (Å) and angles (°)			
Pd–N1	2.1116(14)	N1–Pd–N2	86.67(6)°
Pd–N2	2.1038(14)	Cl1–Pd–Cl2	84.895(18)°
Pd–Cl1	2.3197(4)	N2–Pd–Cl1	168.14(4)°
Pd–Cl2	2.3262(4)	N1–Pd–Cl2	175.64(4)°
		N1–Pd–Cl1	94.80(4)°
		N2–Pd–Cl2	94.52(4)°
		Σ ∠	704.67°

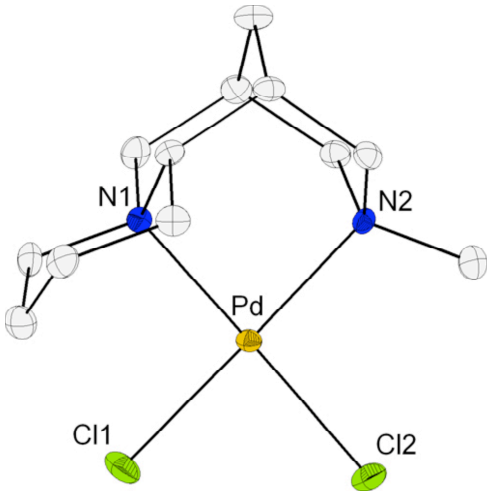

The structure of *N*-ethyl complex **270**, however, is contrary to what would be expected (Figure 4.3.4). It does still have a distorted square planar geometry about the metal center (sum of the six bond angles around the palladium center is 707.01°). However, Cl2 is deflected out of the plane by 8.8°, similar to Pd(sparteine)Cl_2 (**66**, see Figure 4.1.2), instead of displaying a Cl1 deformation as would be expected by a complex with a pseudo-enantiomeric diamine to (–)-sparteine. The cause of this geometric abnormality is still under investigation.

Figure 4.3.4 Structure of *N*-ethyl complex **270**.

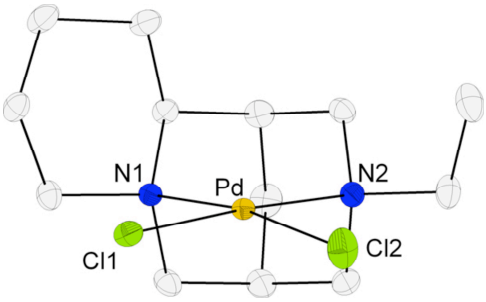

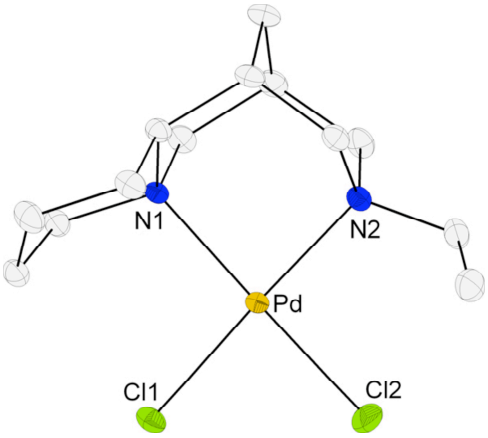

Select bond lengths (Å) and angles (°)			
Pd–N1	2.1294(16)	N1–Pd–N2	86.90(6)°
Pd–N2	2.1114(16)	Cl1–Pd–Cl2	83.73(2)°
Pd–Cl1	2.3254(5)	N2–Pd–Cl1	176.22(5)°
Pd–Cl2	2.3116(5)	N1–Pd–Cl2	171.22(4)°
		N1–Pd–Cl1	95.33(4)°
		N2–Pd–Cl2	93.61(5)°
		Σ ∠	707.01°

Next, these diamines were explored in oxidative kinetic resolutions (Table 4.3.2). For a variety of alkyl group substitutions, selectivity appears to decrease as the *N*-alkyl substituent increases in size (entries 2-6). Notably, *N*-ethyl diamine **260** (entry 3), whose palladium complex (**270**) exhibits the unexpected halide distortion, still provides the same major enantiomer of alcohol as *N*-methyl diamine **248** (entry 2). Both benzyl diamine **261** and secondary amine **268** were completely inactive (entries 7 and 8). Pentadeuterated diamine **271**,[27] a derivative of *N*-methyl diamine **248** postulated to be less prone to oxidation by β-hydride elimination, performs similarly to the undeuterated diamine (cf. entries 2 and 9). Interestingly, tertiary alcohol **267** gives the highest selectivity in the resolution of (±)-1-phenylethanol ((±)-**25**), though oxidations conducted with this ligand are extremely slow.

Table 4.3.2 Diamine substituent screen in the resolution.

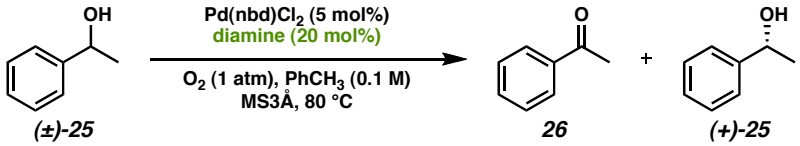

(±)-25 ***26*** ***(+)-25***

entry	diamine	time	conversion[a]	alcohol ee[b]	*s*
1	R = $CH_2C(OH)(CH_3)_2$: ***267***	76 h	27.3%	33.1%	22
2	= Me: ***248***	98 h	45.1%	53.8%	9.6
3	= Et: ***260***	29 h	61.2%	76.2%	7.0
4	= *n*-Bu: ***262***	48 h	54.8%	51.3%	4.0
5	= *i*-Pr: ***265***	145 h	28.4%	18.8%	3.4
6	= Neopentyl: ***263***	24 h	0.6%	–	–
7	= Bn: ***261***	24 h	0.0%	–	–
8	= H: ***268***	76 h	0.0%	–	–
9	***271***	115 h	52.4%	69.9%	9.1
10	(–)-sparteine (***28***)	96 h	59.9%	-98.7%	23

[a] Measured by GC. [b] Measured by chiral HPLC.

Further investigations with this class of ligands were pursued with diamines **248** and **260**. The increased reactivity of catalytic systems with the *N*-ethyl diamine (**260**) were useful for kinetic resolutions of a collection of alcohols in toluene (Table 4.3.3). Cyclohexenol (±)-**119** and cyclopentenol (±)-**111** are able to be resolved with a similar rate and selectivity with diamine **248** (entries 1 and 3) as with (–)-sparteine (entries 2 and 4). Methylcyclopentenol (±)-**120**, on the other hand, is not as efficiently resolved with this (+)-sparteine mimic. Generally, other secondary alcohols studied with this system have poor reactivity and selectivity compared to similar resolutions conducted with (–)-sparteine (**28**).

Table 4.3.3 *N*-Ethyl diamine resolution in toluene with $Pd(nbd)Cl_2$.

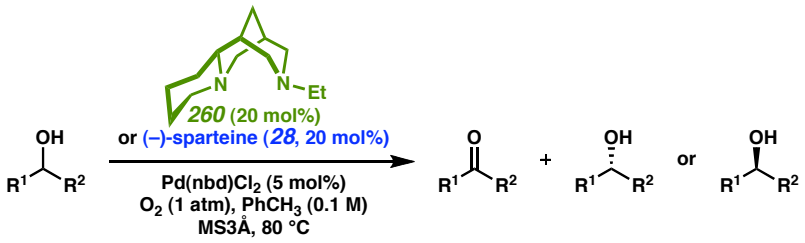

entry	alcohol, major enantiomer	diamine	time	conversion[a]	alcohol ee[b]	*s*
1	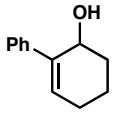 ***(R)-(+)-119***	N-Et diamine (***260***)	23 h	59.2%	98.2%	23
2	***(S)-(–)-119***	(–)-sparteine (***28***)	23 h	60.0%	99.3%	26
3	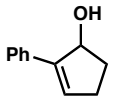 ***(R)-(–)-111***	N-Et diamine (***260***)	23 h	60.8%	99.4%	24
4	***(S)-(+)-111***	(–)-sparteine (***28***)	21 h	57.4%	99.0%	33
5	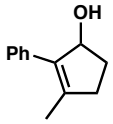 ***(R)-(+)-120***	N-Et diamine (***260***)	10 h	62.3%	98.8%	19
6	***(S)-(–)-120***	(–)-sparteine (***28***)	4 h	52.9%	99.0%	83

[a] Measured by GC. [b] Measured by chiral HPLC.

As is the case with resolutions involving (–)-sparteine, chloroform is an excellent solvent for enantioselective oxidations with *N*-methyl diamine **248**. In addition to the substrates able to be resolved with *N*-ethyl diamine **260** above (entries 1, 3, and 5), a benzylic alcohol (entry 7), and a cyclopropylcarbinyl alcohol (entry 9) are successfully resolved to high enantiomeric excesses. Somewhat lower selectivity is observed with this system compared to the analogous conditions with (–)-sparteine. More disconcerting is the substantially decreased reactivity seen with diamine **248**. Additional research involved improving the reactivity of catalysts derived from these diamines.

Table 4.3.4 *N*-Methyl diamine resolution in chloroform with $Pd(nbd)Cl_2$.

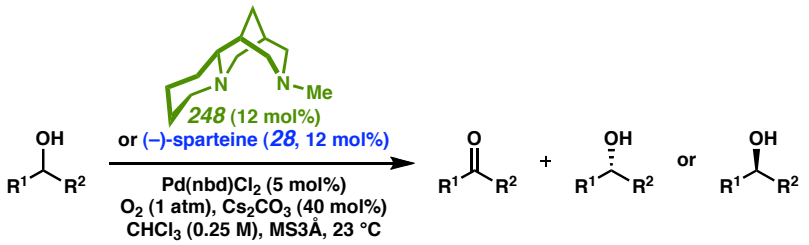

entry	alcohol, major enantiomer		diamine	time	conversion[a]	alcohol ee[b]	*s*
1	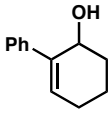	***(R)-(+)-119***	N-Me diamine (***248***)	60 h	59.3%	94.7%	17
2		***(S)-(–)-119***	(–)-sparteine (***28***)	24 h	55.4%	96.8%	33
3	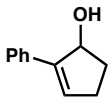	***(R)-(–)-111***	N-Me diamine (***248***)	36 h	59.1%	99.0%	27
4		***(S)-(+)-111***	(–)-sparteine (***28***)	11 h	58.4%	98.8%	28
5	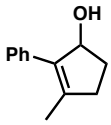	***(R)-(+)-120***	N-Me diamine (***248***)	24 h	68.1%	99.5%	14
6		***(S)-(–)-120***	(–)-sparteine (***28***)	9 h	57.9%	96.9%	23
7	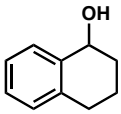	***(R)-(–)-82***	N-Me diamine (***248***)	48 h	61.8%	99.5%	23
8		***(S)-(+)-82***	(–)-sparteine (***28***)	24 h	58.0%	98.4%	28
9	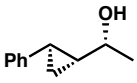	***(–)-126***	N-Me diamine (***248***)	107 h	50.3%	71.4%	12
10		***(+)-126***	(–)-sparteine (***28***)	25 h	58.6%	99.0%	28

[a] Measured by GC. [b] Measured by chiral HPLC.

The selectivity observed with diamine **248** is in line with the selectivity model proposed for the oxidative kinetic resolution with (–)-sparteine (Scheme 4.3.5).[8] For $Pd(sparteine)Cl_2$ (**66**), faster reacting alcohol (–)-**111** proceeds through intermediate **141** to undergo β-hydride elimination via transition state **142** to provide ketone **143**. Conversely for *N*-methyl complex **269**, alcohol (+)-**111** is the faster reacting enantiomer. Alcohol coordination generates intermediate palladium alkoxide **272**, which undergoes β-hydride elimination via transition state **273** to provide ketone **143** as well.

Scheme 4.3.5 Comparison of selectivity with different diamine ligands.

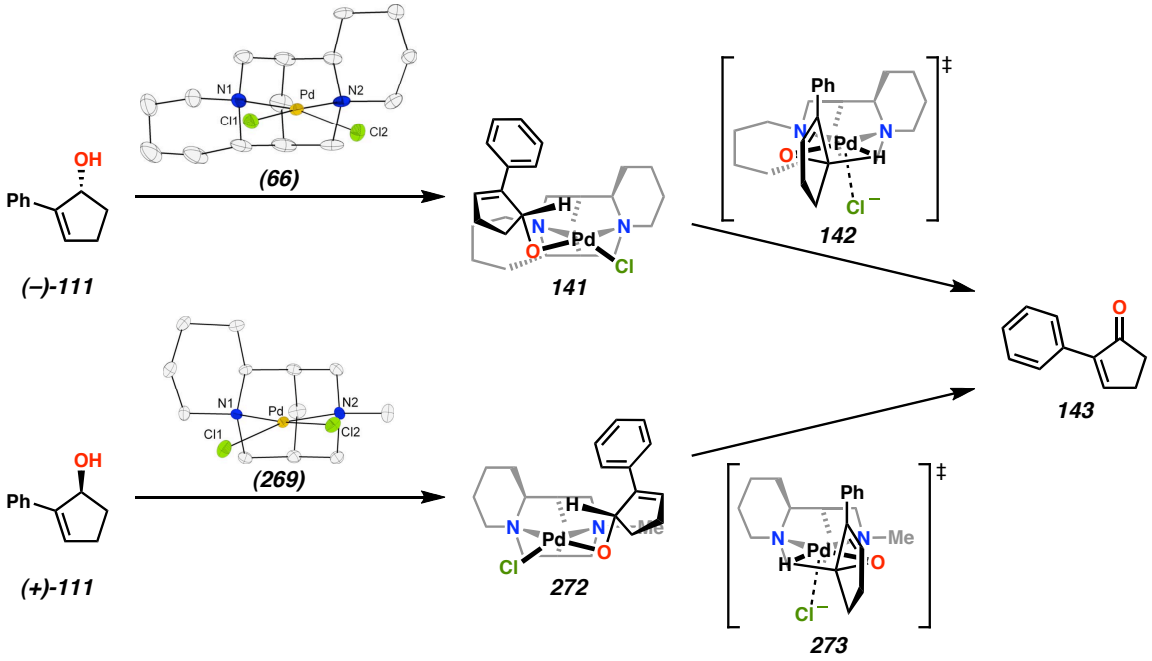

4.3.3 Alternative Diamine with $PdBr_2$ in the Oxidative Kinetic Resolution

The decreased reactivity of catalytic systems with the (–)-cytisine-based diamines led us to apply insights gained from the previous counterion studies to improve oxidation rates. Thus, dibromide complex **274** was prepared by treatment of dibromide precursor **244** with diamine **248** in dichloromethane (Scheme 4.3.6). This complex was recrystallized to provide crystals suitable for X-ray analysis (Figure 4.3.5), which reveals a distorted square planar geometry (sum of the six bond angles around palladium is 701.69°). The Br1 deflection is large (14.2°), but comparable with the deformation of Br2 of Pd(sparteine)Br_2 (**242**, 14.0°). Based on this larger deflection relative to dichloride complex **66** (11.9°), we anticipated that dibromide complex **274** would be a highly active catalyst for the oxidative kinetic resolution.

Scheme 4.3.6 Synthesis of dibromide complex **274**.

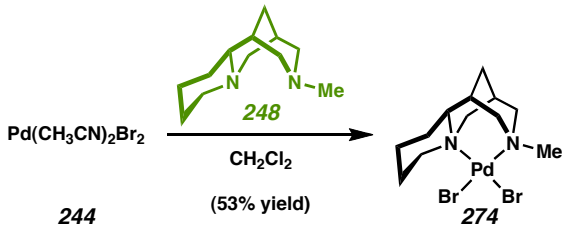

Figure 4.3.5 Structure of dibromide complex **274**.

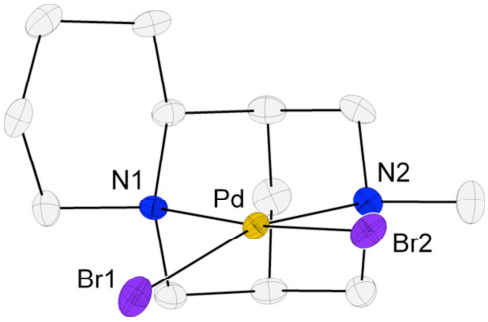

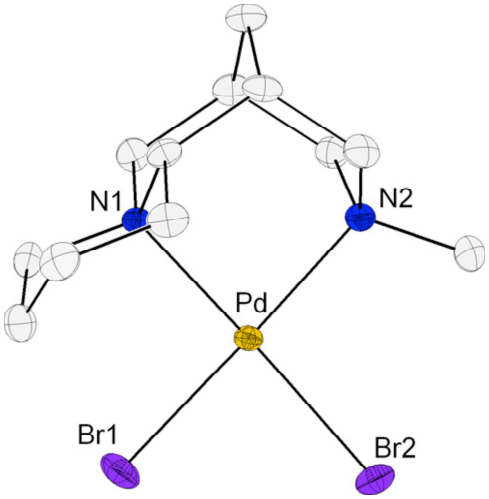

Select bond lengths (Å) and angles (°)			
Pd–N1	2.126(2)	N1–Pd–N2	86.46(8)°
Pd–N2	2.117(2)	Br1–Pd–Br2	84.449(12)°
Pd–Br1	2.4463(3)	N2–Pd–Br1	165.81(6)°
Pd–Br2	2.4513(3)	N1–Pd–Br2	174.56(6)°
		N1–Pd–Br1	95.17(6)°
		N2–Pd–Br2	95.24(6)°
		Σ ∠	701.69°

Diamine **248** was then explored in enantioselective oxidations of (±)-1-phenylethanol ((±)-**25**) with $Pd(CH_3CN)_2Br_2$ (**244**) as the dibromide catalyst precursor (Table 4.3.5). Analogous to the (–)-sparteine complexes, the catalyst derived from dibromide **244** is substantially more active than those derived from dichloride salts, while maintaining similar selectivity factors (cf. entries 1 and 4). An excess of diamine **248** is required to maintain viable catalysts (entries 4-7), though a large excess leads to some catalyst deactivation (entries 2 and 3). Use of the preformed dibromide complex (**274**) provides similar rates and selectivity (cf. entries 5 and 8). For operational simplicity, in

situ catalyst generation is preferred. Reactions maintained at 20 °C (entry 9) provide slightly improved selectivity and more consistent results than those at 23 °C (entry 5).

Table 4.3.5 Optimization of with *N*-methyl diamine and $PdBr_2$ sources.

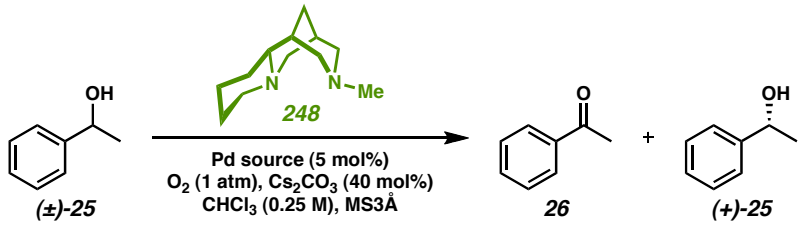

(±)-25 26 (+)-25

entry	Pd source	temperature	mol% diamine ***248***	time	conversion[a]	alcohol ee[b]	*s*
1	$Pd(nbd)Cl_2$	23 °C	12	41 h	29.9%	37.0%	20
2	$Pd(CH_3CN)_2Br_2$ (***244***)	23 °C	20	45 h	31.0%	38.9%	20
3	$Pd(CH_3CN)_2Br_2$ (***244***)	23 °C	15	35 h	39.9%	56.2%	21
4	$Pd(CH_3CN)_2Br_2$ (***244***)	23 °C	12	32 h	58.0%	96.1%	21
5	$Pd(CH_3CN)_2Br_2$ (***244***)	23 °C	10	35 h	55.5%	92.5%	22
6[c]	$Pd(CH_3CN)_2Br_2$ (***244***)	23 °C	7	24 h	41.6%	61.0%	24
7[c]	$Pd(CH_3CN)_2Br_2$ (***244***)	23 °C	5	35 h	19.3%	21.6%	24
8	$Pd(diamine)Br_2$ (***274***)	23 °C	5	41 h	56.1%	93.6%	22
9	$Pd(CH_3CN)_2Br_2$ (***244***)	20 °C	10	30 h	57.6%	97.1%	25

[a] Measured by GC. [b] Measured by chiral HPLC. [c] Pd black observed.

With optimized conditions in hand, we examined the scope of this transformation (Table 4.2.11). A number of benzylic alcohols are able to be resolved with good selectivity with this method (entries 1-5). Furthermore, allylic alcohols (entries 6-10), including several alcohols not successfully resolved with diamine **248** and $Pd(nbd)Cl_2$ (entries 9 and 10), are obtained with high enantiomeric excesses in shorter times. Cyclopropylcarbinyl alcohols containing three contiguous stereocenters are also resolved to high ee (entries 11 and 12). To further improve the practicality of the method, several resolutions were conducted under an atmosphere of ambient air. As seen in entries 2 and 4, kinetic resolutions under air perform nearly identically to those under an atmosphere of molecular oxygen (entries 1 and 3).

Table 4.3.6 Scope with dibromide catalysts of *N*-methyl diamine.

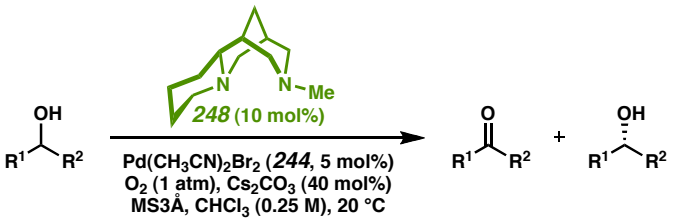

entry	alcohol, major enantiomer	time	conversion[a] (yield)[b]	alcohol ee[c]	*s*
1	 *(+)-25*	30 h	57.6% (40%)	97.1%	25
2[d]		34 h	57.9%	96.4%	22
3	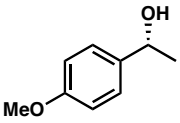 *(+)-67*	30 h	60.4%	97.7%	19
4[d]		34 h	61.2%	98.1%	19
5	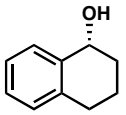 *(–)-82*	24 h	60.9% (38%)	90.2%	11
6	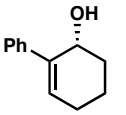 *(+)-119*	46 h	56.8% (43%)	90.7%	17
7	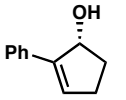 *(–)-111*	12 h	55.0%	94.1%	27
8	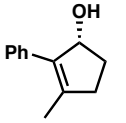 *(+)-120*	18 h	63.2%	94.4%	12
9	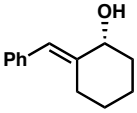 *(+)-105*	46 h	59.3% (39%)	90.6%	13
10	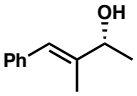 *(–)-104*	35 h	62.6%	92.0%	11
11	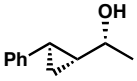 *(–)-126*	32 h	59.0% (40%)	90.2%	13
12	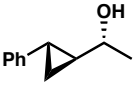 *(+)-128*	35 h	62.3%	90.0%	10

[a] Measured by GC or ^{1}H NMR. [b] Isolated yield of enantioenriched alcohol. [c] Measured by chiral HPLC. [d] Performed under ambient air.

4.4 Conclusion

Extensive counterion and neutral ligand studies have provided us with a thorough understanding of the factors that contribute to the reactivity and selectivity of the oxidative kinetic resolution of secondary alcohols. Solid-state X-ray crystallographic analysis proved vital to these studies, leading to many valuable insights. As a result, several greatly improved catalyst systems have been developed. Counterion investigations have led to the discovery of dibromide complexes of palladium with (–)-sparteine as highly active catalysts for the enantioselective aerobic oxidation of a broad range of substrates, including numerous examples of alcohols not resolved efficiently with previously developed Pd(sparteine)Cl_2 conditions. Broad surveys of neutral ligands have emphasized the unique ability of sparteine-like diamines to promote palladium-catalyzed oxidation, leading to diamines developed by O'Brien as excellent mimics of (+)-sparteine. These diamines have been employed successfully in the oxidative kinetic resolution, affording alcohols in the enantiomeric series opposite to that obtained with (–)-sparteine and greatly increasing the synthetic utility of this method.

4.5 Experimental Section

4.5.1 Materials and Methods

Pd(sparteine)Cl_2 (**66**),[8] Pd(sparteine)$(OAc)_2$ (**231**),[9] Pd(sparteine)$(TFA)_2$ (**241**),[13] Pd(sparteine)Br_2 (**242**),[1] Pd(COD)Br_2 (**245**), and Pd(nbd)Br_2 (**246**)[28] were prepared as previously reported. Palladium bromide was purchased from Strem Chemicals. (+)- And (–)-2'-methoxy-1,1'-binaphthyl-2-ol were prepared by the method of Xi.[12] (+)-1-Phenylethanol ((+)-**25**) was purchased from Acros Organics. (±)-(*E*)-3-Methyl-4-phenyl-3-buten-2-ol ((±)-**104**) was prepared by the method of West.[29] Diamines **248**,[22,23] **260**, **262**, **263**,[24] **261**, **265**,[25] and **271**[27] were prepared as previously described. Solvents were dried by passage through an activated alumina column under argon. Powdered 3Å molecular sieves were stored in a 120 °C drying oven until immediately prior to use. Other chemicals were prepared as described below, prepared as described in Chapter 3, or purchased from the Sigma-Aldrich Chemical Company and used as received. Unless stated otherwise, reactions were performed in flame-dried glassware sealed with rubber septa under a nitrogen atmosphere using dry, deoxygenated solvents. Liquids and solutions were transferred via syringe. Reaction temperatures were controlled using an IKAmag temperature modulator (heating) or a VWR 1160 refrigerated circulating bath (cooling). Thin-layer chromatography (TLC) was conducted with E. Merck silica gel 60 F254 pre-coated plates (0.25 mm) and visualized using a combination of UV at 254 nm, *p*-anisaldehyde, and potassium permanganate staining. ICN silica gel (particle size 32-63 μm) or SiliCycle Silia*Flash* P60 Academic silica gel (particle size 40-63 μm; pore diameter 60 Å) was used for flash column chromatography. Analytical achiral GC was performed on an Agilent 6850 GC with FID detector using an Agilent DB-WAX (30.0 m

x 0.25 mm) column at 1.0 mL/min He carrier gas flow. Chiral GC was performed on an Agilent 6850 GC with FID detector using a Chiraldex GTA column (30.0 m x 0.25 mm, purchased from Bodman Industries) at 1.0 mL/min He carrier gas flow. Analytical chiral HPLC was performed with an Agilent 1100 Series HPLC utilizing a Chiralpak AD, Chiralcel OD-H, Chiralcel OJ, or Chiralcel OB-H column (each is 4.6 mm x 25 cm) obtained from Daicel Chemical Industries, Ltd with visualization at 254 nm at 1.0 mL/min mobile phase. ^{1}H NMR spectra were recorded on a Varian Mercury 300 or 500 instrument (at 300 or 500 MHz, respectively) and are reported relative to Me_4Si (δ 0.0). Data for ^{1}H NMR spectra are reported in terms of chemical shift (δ ppm), multiplicity, coupling constant (Hz), and integration. ^{13}C NMR spectra were recorded on a Varian Mercury 300 or 500 instrument (at 75 or 126 MHz, respectively) and are reported relative to Me_4Si (δ 0.0). Data for ^{13}C NMR spectra are reported in terms of chemical shift (δ ppm). Melting points were determined on a Thomas-Hoover melting point apparatus and are uncorrected. Elemental analyses were carried out by Desert Analytics Laboratory, Tuscon, AZ. X-ray crystal structure analyses were obtained from the California Institute of Technology X-Ray Crystallography Laboratory. The absolute configurations of resolved alcohols were assigned based on comparisons of optical rotations to literature values or by analogy.

4.5.2 Preparation of Palladium Complexes and Diamines

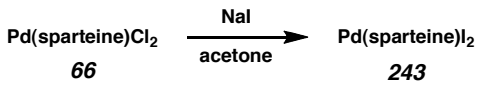

Diiodo(sparteine)palladium(II) (243). Sodium iodide (134 mg, 0.89 mmol, 2.1 equiv) was added to a suspension of complex **66** (175 mg, 0.43 mmol, 1.0 equiv) in

acetone (10 mL). The dark mixture was stirred at 23 °C for 30 min, after which the solvent was removed under reduced pressure. The solid was washed with copious amounts of H_2O followed by pentane to afford **243** as a dark purple solid: ^{1}H NMR (500 MHz, $CDCl_3$) δ 4.43 (app. dd, *J* = 12.5, 3.2 Hz, 1H), 4.33 (br. d, *J* = 11.7 Hz, 1H), 4.19 (ddd, *J* = 14.4, 13.1, 3.0 Hz, 1H), 3.92 (dt, *J* = 12.4, 2.4 Hz, 1H), 3.75-3.59 (comp. m, 2H), 2.97 (dd, *J* = 12.9, 3.4 Hz, 1H), 2.93-2.79 (comp. m, 2H), 2.54 (dd, *J* = 12.4, 3.1Hz, 1H), 2.17-1.37 (comp. m, 16H); ^{13}C NMR (126 MHz, $CDCl_3$) δ 72.2, 70.2, 66.5, 64.7, 63.8, 48.9, 35.0, 34.9, 29.5, 28.1, 27.3, 26.9, 24.3, 23.6, 21.8; IR (thin film/NaCl): 2935, 1440, 913, 728 cm^{-1}; HRMS-FAB (*m/z*): $[M]^+$ calcd for $[C_{15}H_{26}N_2I_2Pd]^+$, 593.9221; found, 593.9242.

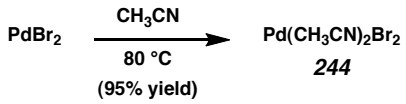

Dibromobis(acetonitrile)palladium(II) (244). Palladium bromide (532 mg, 2.0 mmol, 1.0 equiv) was added to acetonitrile (40 mL). The mixture was heated to 80 °C for 1.5 h. Once the solution became clear and orange-red, the reaction was cooled to 23 °C. The mixture was concentrated under reduced pressure to a volume of about 5 mL and then triturated with Et_2O (15 mL). The orange-red solid was filtered, washed with Et_2O (2 x 15 mL), and dried under vacuum to afford **244** (661 mg, 95% yield).

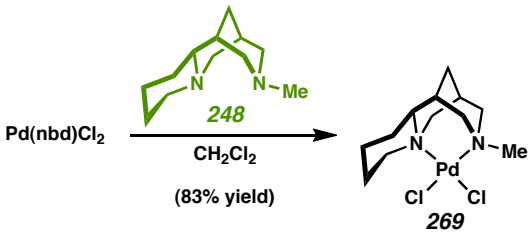

Dichloride Complex 269. To a solution of freshly distilled diamine **248**[23] (194 mg, 1.0 mmol, 1.0 equiv) in CH_2Cl_2 (20 mL) was added $Pd(nbd)Cl_2$ (269 mg, 1.0 mmol, 1.0 equiv). The reaction was allowed to stir 1 h. Then, the volatiles were removed under reduced pressure. The resulting solid was washed with pentane (3 x 5 mL) to afford **269** (310 mg, 83% yield) as a reddish-brown solid: mp 183-185 °C (dec.); ^{1}H NMR (300 MHz, $CDCl_3$) δ 4.30 (dq, *J* = 12.4, 1.7 Hz, 1H), 4.11 (dt, *J* = 12.8, 2.1 Hz, 1H), 3.95 (br. d, *J* = 12.0 Hz, 1H), 3.33 (dq, *J* = 13.0, 1.8 Hz, 1H), 3.10 (qd, *J* = 12.6, 3.6 Hz, 1H), 2.91-2.72 (m, 1H), 2.67 (s, 3H), 2.43 (dd, *J* = 12.6, 2.8 Hz, 1H), 2.38-2.27 (comp. m, 2H), 2.07 (dd, *J* = 13.1, 3.1 Hz, 1H), 2.04-1.94 (m, 1H), 1.91-1.73 (comp. m, 5H), 1.64-1.39 (comp. m, 3H); ^{13}C NMR (75 MHz, $CDCl_3$) δ 69.6, 64.7, 64.4, 64.1, 58.8, 57.0, 34.0, 32.8, 30.2, 29.3, 25.0, 24.2; IR (thin film/NaCl): 2953, 2856, 1454, 1009 cm^{-1}; HRMS-FAB (*m/z*): $[M-Cl]^+$ calcd for $[C_{12}H_{22}N_2ClPd]^+$, 337.0510; found, 337.0503; A single crystal suitable for X-ray analysis was grown by slow diffusion of heptane into a saturated $CHCl_3$ solution of **269**.

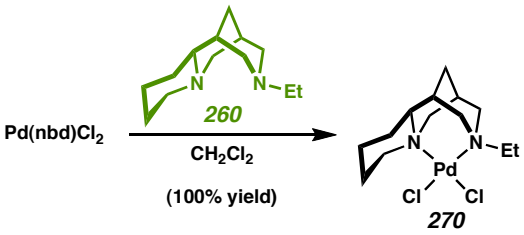

Dichloride Complex 270. To a solution of freshly distilled diamine **260** (208 mg, 1.0 mmol, 1.0 equiv) in CH_2Cl_2 (20 mL) was added Pd(nbd)Cl_2 (269 mg, 1.0 mmol, 1.0 equiv). The reaction was allowed to stir 1 h. Then, the volatiles were removed under reduced pressure. The resulting solid was washed with pentane (3 x 5 mL) and then hot filtered in $CHCl_3$ (200 mL). Heptane was layered over the filtrate, and the biphasic mixture was allowed to stand 4 d. The mixture was then filtered to afford **270** (386 mg, 100% yield) as an orange-brown solid: mp 177-179 °C (dec.); ^{1}H NMR (300 MHz, $CDCl_3$) δ 4.45 (app. d, *J* = 12.6 Hz, 1H), 4.34 (dt, *J* = 12.7, 2.1 Hz, 1H), 4.01 (br. d, *J* = 11.7 Hz, 1H), 3.77 (dq, *J* = 12.0, 6.9 Hz, 1H), 3.25 (app. d, *J* = 12.4 Hz, 1H), 2.84-2.63 (comp. m, 2H), 2.50-2.36 (comp. m, 3H), 2.09-1.70 (comp. m, 8H), 1.65-1.38 (comp. m, 3H), 1.32 (t, *J* = 6.9 Hz, 3H); ^{13}C NMR (75 MHz, $CDCl_3$) δ 69.0, 64.7, 64.1, 63.9, 61.1, 54.0, 33.5, 33.1, 30.2, 29.5, 25.0, 24.2, 12.7; IR (thin film/NaCl): 2856, 1460, 1033, 742 cm^{-1}; HRMS-FAB (*m*/*z*): $[M]^+$ calcd for $[C_{13}H_{24}N_2Cl_2Pd]^+$, 386.0356; found, 386.0338; A single crystal suitable for X-ray analysis was grown by slow diffusion of heptane into a saturated $CHCl_3$ solution of **270**.

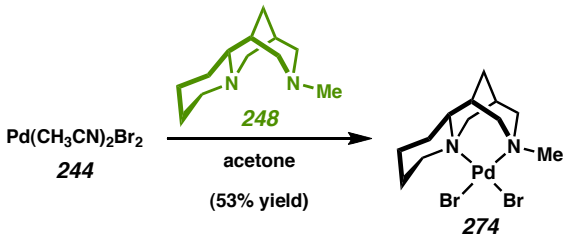

Dibromide Complex 274. To a solution of **244** (69.7 mg, 0.20 mmol, 1.0 equiv) in acetone (2 mL) was added a solution of freshly distilled diamine **248** (38.9 mg, 0.20 mmol, 1.0 equiv) in acetone (2 mL). The reaction was allowed to stir 1 h, after which Et_2O (4 mL) was layered over the mixture. The solid was filtered and washed with Et_2O (2 x 2 mL). 1,2-Dichloroethane (4 mL) was added to the solid, and the mixture was stirred vigorously for 4 h. After filtration of insoluble material, the filtrate was concentrated under reduced pressure to afford **274** (48.4 mg, 53% yield) as a brown solid: mp 197-199 °C (dec.); ^{1}H NMR (300 MHz, $CDCl_3$) δ 4.30 (dq, *J* = 13.0, 1.9 Hz, 1H), 4.15 (br. d, *J* = 12.1 Hz, 1H), 4.04 (dt, *J* = 12.6, 2.2 Hz, 1H), 3.30 (dq, *J* = 12.9, 1.8 Hz, 1H), 3.15 (qd, *J* = 12.3, 3.7 Hz, 1H), 2.95-2.76 (m, 1H), 2.87 (s, 3H), 2.59-2.50 (m, 1H), 2.43 (dd, *J* = 12.5, 2.8 Hz, 1H), 2.37-2.29 (m, 1H), 2.25 (dd, *J* = 13.0, 3.0 Hz, 1H), 2.05 (dd, *J* = 13.1, 3.2 Hz, 1H), 2.02-1.73 (comp. m, 5H), 1.64-1.41 (comp. m, 3H); ^{13}C NMR (75 MHz, $CDCl_3$) δ 69.7, 65.2, 64.7, 64.2, 59.8, 58.8, 34.1, 32.8, 30.1, 29.3, 25.8, 24.2; IR (thin film/NaCl): 2943, 1455, 1008 cm^{-1}; HRMS-FAB (*m*/*z*): $[M]^+$ calcd for $[C_{12}H_{22}Br_2N_2Pd]^+$, 459.9189; found, 459.9198. A single crystal suitable for X-ray analysis was grown by slow diffusion of hexanes into a saturated $CHCl_3$ solution of **274**.

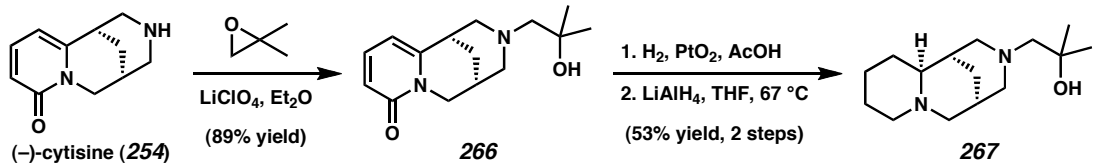

Diamine 267. To $LiClO_4$ (oven- and flame-dried, 4.26 g, 40 mmol, 10.0 equiv) was added Et_2O (8 mL). The mixture was stirred vigorously for 15 min, then isobutylene oxide (391 μL, 317 mg, 4.4 mmol, 1.1 equiv) and (–)-cytisine[23] (**254**, 761 mg, 4.0 mmol, 1.0 equiv) were added. After stirring the mixture vigorously for 50 h, the reaction was diluted with H_2O (30 mL). The biphasic mixture was extracted with CH_2Cl_2 (4 x 30 mL). The combined organic layers were dried over Na_2SO_4 and filtered. The filtrate was concentrated under reduced pressure to afford pyridone **266** (935 mg, 89% yield) as a tan solid: ^{1}H NMR (300 MHz, $CDCl_3$) δ 7.28 (dd, *J* = 9.1, 6.8 Hz, 1H), 6.44 (dd, *J* = 9.1, 1.3 Hz, 1H), 6.00 (dd, *J* = 6.8, 1.3 Hz, 1H), 4.17 (d, *J* = 15.5 Hz, 1H), 3.89 (dd, *J* = 15.5, 6.5 Hz, 1H), 3.04-2.93 (comp. m, 3H), 2.71-2.62 (comp. m, 2H), 2.42 (br. s, 1H), 2.21 (s, 2H), 1.95-1.86 (m, 1H), 1.82-1.72 (comp. m, 2H), 0.97 (s, 3H), 0.94 (s, 3H). The crude pyridone was used in the next step without further purification.

To crude pyridone **266** was added AcOH (glacial, 12 mL) and PtO_2 (81 mg, 0.36 mmol, 0.10 equiv). The reaction was then stirred under a balloon of H_2 (1 atm) for 48 h. The black mixture was filtered through Celite (MeOH eluent), and the filtrate was concentrated under reduced pressure. $PhCH_3$ (50 mL) was added, and the solution was concentrated under reduced pressure to effect azeotropic removal of traces of AcOH and afford the crude amide as a slightly yellow oil, which was used in the next step without further purification.

A solution of the crude amide in THF (16 mL) was cooled to 0 °C. $LiAlH_4$ (811 mg, 21.4 mmol, 6.0 equiv) was added in small portions. The mixture was heated to

reflux for 22 h, then cooled to 0 °C. Saturated aq Na_2SO_4 was added dropwise until bubbling ceased. The reaction was allowed to warm to 23 °C and stirred vigorously for 2 h. The mixture was diluted with CH_2Cl_2 (50 mL) and aq NaOH (10% w/v, 50 mL) and stirred 2 h. The mixture was then filtered, and the layers separated. The aqueous layer was extracted with CH_2Cl_2 (3 x 50 mL). The combined organic layers were dried over Na_2SO_4, filtered, and the filtrate concentrated under reduced pressure. Bulb-to-bulb distillation (0.2 torr, 170-190 °C) afforded diamine **267** (477 mg, 53% yield) as a colorless oil: ^{1}H NMR (500 MHz, $CDCl_3$) δ 5.73 (br. s, 1H), 3.05 (d, *J* = 11.1 Hz, 1H), 2.98 (d, *J* = 10.7 Hz, 1H), 2.89 (d, *J* = 11.3 Hz, 1H), 2.81-2.75 (m, 1H), 2.72 (dt, *J* = 10.7, 2.2 Hz, 1H), 2.61 (dd, *J* = 11.2, 2.5 Hz, 1H), 2.30-2.21 (comp. m, 3H), 1.81-1.50 (comp. m, 7H), 1.46-1.42 (m, 1H), 1.37-1.20 (comp. m, 3H), 1.18 (s, 3H), 1.16 (s, 3H); ^{13}C NMR (126 MHz, $CDCl_3$) δ 68.9, 66.7, 66.3, 60.8, 59.6, 57.4, 55.4, 36.0, 34.5, 31.3, 30.5, 29.9, 29.2, 25.9, 25.1; IR (thin film/NaCl) 3252, 2931, 2758, 1166 cm^{-1}; HRMS-FAB (*m/z*): $[M+H]^+$ calcd for $[C_{15}H_{29}N_2O]^+$, 253.2280; found 253.2280; $[\alpha]^{24}_D$ +27.1° (*c* 1.0, $CHCl_3$).

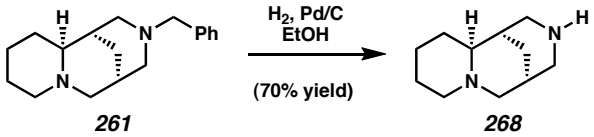

261 *268*

Diamine 268. To benzyl diamine **261**[25] (472 mg, 1.75 mmol, 1.0 equiv) was added EtOH (absolute, 8.8 mL) and then Pd/C (10% w/w, 186 mg, 0.18 mmol Pd, 0.10 equiv). The reaction was then stirred under a balloon of H_2 (1 atm) for 22 h. The mixture was then filtered through Celite (EtOH eluent). The filtrate was concentrated under reduced pressure and purified by bulb-to-bulb distillation (1-2 torr, 100-130 °C) to yield a colorless oil. To this oil was added Et_2O (10 mL), then HCl (2 M in Et_2O, 1.39 mL, 2.77

mmol, 1.6 equiv) dropwise. A white solid formed immediately. After stirring 30 min, the solid was collected by filtration, washed quickly with Et_2O (3 x 5 mL) and dissolved in CH_2Cl_2 (10 mL). NaOH (10% w/v aq, 10 mL) was added dropwise. The layers were separated, and the aqueous layer was extracted with CH_2Cl_2 (3 x 10 mL). The combined organic layers were dried over Na_2SO_4, filtered, and the filtrate concentrated under reduced pressure. Bulb-to-bulb distillation (1-2 torr, 110-125 °C) afforded diamine **268** (264 mg, 70% yield) as an oil, which solidified on standing to a white solid: ^{1}H NMR (500 MHz, $CDCl_3$) δ 3.22 (app. dt, *J* = 13.9, 2.3 Hz, 1H), 3.03 (br. d, *J* = 13.5 Hz, 1H), 2.94 (app. dt, *J* = 13.5, 2.5 Hz, 1H), 2.86 (dt, *J* = 11.0, 2.3 Hz, 1H), 2.76-2.70 (comp. m, 2H), 2.40 (dt, *J* = 11.0, 2.5 Hz, 1H), 2.11 (app. dt, *J* = 11.2, 2.6 Hz, 1H), 1.87 (dtd, *J* = 12.2, 3.1, 2.2 Hz, 1H), 1.80-1.66 (comp. m, 3H), 1.62-1.47 (comp. m, 4H), 1.43-1.37 (m, 1H), 1.34-1.24 (comp. m, 2H); ^{13}C NMR (126 MHz, $CDCl_3$) δ 66.4, 61.9, 57.5, 52.7, 48.5, 35.2, 34.7, 30.7, 30.3, 26.2, 24.9; IR (thin film/NaCl) 3387, 2930, 1654, 1442 cm^{-1}; HRMS-FAB (*m/z*): [M+H]$^+$ calcd for $[C_{11}H_{21}N_2]^+$, 181.1705; found 181.1703; $[\alpha]^{24}_D$ +21.51° (*c* 1.0, $CHCl_3$).

4.5.3 General Procedures

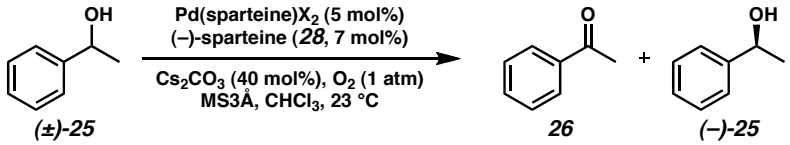

Kinetic Resolution Conditions with Pd(sparteine)X_2 and Cs_2CO_3 in $CHCl_3$ under O_2.[11] To an oven dried reaction tube with stir bar was added 3Å molecular sieves (250 mg). After cooling, Pd(sparteine)X_2 (0.025 mmol, 0.05 equiv), followed by $CHCl_3$ (1 mL)[30] and then (–)-sparteine (**28**, 8.0 μL, 0.035 mmol, 0.07 equiv) were added. The

reaction tube was cooled to –78 °C, then vacuum evacuated and purged with O_2 (3x). The reaction was allowed to warm to 23 °C and stirred vigorously under a balloon of O_2 (1 atm) for 15 min. Finely powdered Cs_2CO_3 (65.2 mg, 0.20 mmol, 0.40 equiv) was added, followed by a solution of (±)-1-phenylethanol ((±)-**25**, 60.3 μL, 0.50 mmol, 1.0 equiv) and tridecane (36.6 μL, 0.15 mmol, 0.30 equiv) in $CHCl_3$ (1 mL). The reaction was allowed to proceed under O_2 atmosphere at 23 °C. Aliquots were filtered through a small plug of silica gel (Et_2O eluent), evaporated, and analyzed by GC for conversion and chiral HPLC for alcohol ee. Purification of **26** and (–)-**25** was accomplished by direct chromatography of the crude reaction mixture.

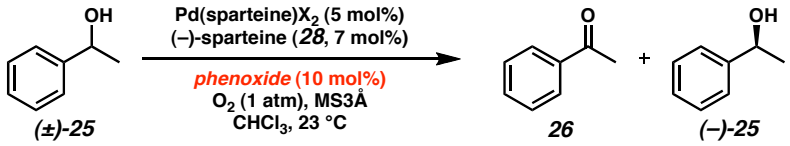

Kinetic Resolution Conditions with Pd(sparteine)X_2 and Phenoxides. To an oven dried reaction tube with stir bar was added 3Å molecular sieves (250 mg), Pd(sparteine)X_2 (0.025 mmol, 0.05 equiv), phenoxide[31] (0.05 mmol, 0.10 equiv), $CHCl_3$ (1 mL),[30] and **28** (8.0 μL, 0.035 mmol, 0.07 equiv). The reaction tube was cooled to –78 °C, then vacuum evacuated and purged with O_2 (3x). The reaction was allowed to warm to 23 °C and stirred vigorously under a balloon of O_2 (1 atm) for 1 h. A solution of (±)-**25** (60.3 μL, 0.50 mmol, 1.0 equiv) and tridecane (36.6 μL, 0.15 mmol, 0.30 equiv) in $CHCl_3$ (1 mL) was added. The reaction was allowed to proceed under O_2 atmosphere at 23 °C. Aliquots were filtered through a small plug of silica gel (Et_2O eluent), evaporated, and analyzed by GC for conversion and chiral HPLC for alcohol ee. Purification of **26** and (–)-**25** was accomplished by direct chromatography of the crude reaction mixture.

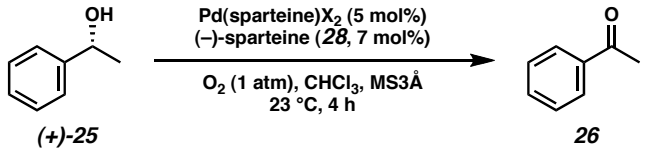

Single Enantiomer Rate Experiments with Various Pd(sparteine)X_2 Sources. To an oven dried reaction tube with stir bar was added 3Å molecular sieves (250 mg). After allowing the tube to cool, Pd(sparteine)X_2 (0.025 mmol, 0.05 equiv) was added, followed by $CHCl_3$ (1 mL)[30] and then **28** (8.0 μL, 0.035 mmol, 0.07 equiv). The reaction tube was cooled to –78 °C, then vacuum evacuated and purged with O_2 (3x). The reaction was allowed to warm to 23 °C and stirred vigorously under a balloon of O_2 (1 atm) for 15 min. A solution of (+)-**25** (60.4 μL, 0.50 mmol, 1.0 equiv) and tridecane (36.6 μL, 0.15 mmol, 0.30 equiv) in $CHCl_3$ (1 mL) was added. The reaction was allowed to proceed under O_2 atmosphere at 23 °C. Aliquots were filtered through a small plug of silica gel (Et_2O eluent), evaporated, and analyzed by GC for conversion to acetophenone (**26**).

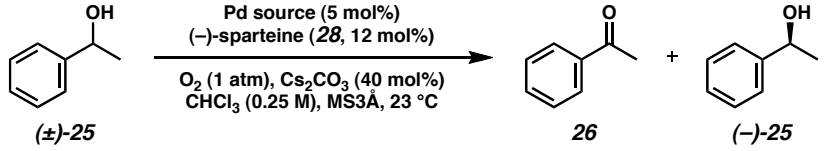

Screening of $PdBr_2$ Sources in $CHCl_3$. To an oven dried reaction tube with stir bar was added 3Å molecular sieves (250 mg). After allowing the tube to cool, the palladium source (0.025 mmol, 0.05 equiv) was added, followed by $CHCl_3$ (1 mL)[30] and then **28** (13.8 μL, 0.060 mmol, 0.12 equiv).[32] The reaction tube was cooled to –78 °C, then vacuum evacuated and purged with O_2 (3x). The reaction was allowed to warm to

23 °C and stirred vigorously under a balloon of O_2 (1 atm) for 15 min. Finely powdered Cs_2CO_3 (65.2 mg, 0.20 mmol, 0.40 equiv) was added, followed by a solution of (±)-**25** (60.3 μL, 0.50 mmol, 1.0 equiv) and tridecane (36.6 μL, 0.15 mmol, 0.30 equiv) in $CHCl_3$ (1 mL). The reaction was allowed to proceed under O_2 atmosphere at 23 °C. Aliquots were filtered through a small plug of silica gel (Et_2O eluent), evaporated, and analyzed by GC for conversion and chiral HPLC for alcohol ee.

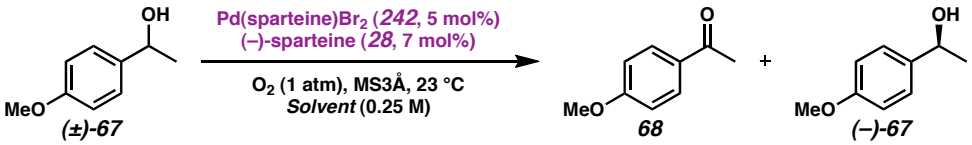

Solvent Screen with Pd(sparteine)Br_2. To an oven dried reaction tube with stir bar was added 3Å molecular sieves (250 mg). After allowing the tube to cool, Pd(sparteine)Br_2 (**242**, 12.5 mg, 0.025 mmol, 0.05 equiv) was added, followed by the solvent (1 mL) and then **28** (8.0 μL, 0.035 mmol, 0.07 equiv). The reaction tube was cooled to –78 °C, then vacuum evacuated and purged with O_2 (3x). The reaction was allowed to warm to 23 °C and stirred vigorously under a balloon of O_2 (1 atm) for 15 min. A solution of (±)-**67** (76.1 mg, 0.50 mmol, 1.0 equiv) and tridecane (36.6 μL, 0.15 mmol, 0.30 equiv) in the solvent (1 mL) was added. The reaction was allowed to proceed under O_2 atmosphere at 23 °C. Aliquots were filtered through a small plug of silica gel (Et_2O eluent), evaporated, and analyzed by GC for conversion and chiral HPLC for alcohol ee.

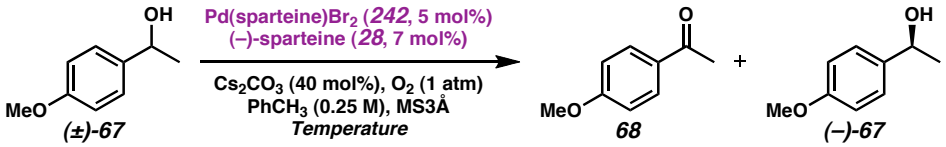

Kinetic Resolution Conditions with Pd(sparteine)Br_2 (242) and O_2 in $PhCH_3$. To an oven dried reaction tube with stir bar was added 3Å molecular sieves (250 mg). After allowing the tube to cool, Pd(sparteine)Br_2 (**242**, 12.5 mg, 0.025 mmol, 0.05 equiv) was added, followed by the $PhCH_3$ (1 mL) and then **28** (8.0 μL, 0.035 mmol, 0.07 equiv). The reaction tube was cooled to –78 °C, then vacuum evacuated and purged with O_2 (3x). The reaction was warmed to the appropriate temperature (23 or 60 °C) and stirred vigorously under a balloon of O_2 (1 atm) for 15 min. A solution of (±)-**67** (76.1 mg, 0.50 mmol, 1.0 equiv) and tridecane (36.6 μL, 0.15 mmol, 0.30 equiv) in $PhCH_3$ (1 mL) was added. The reaction was allowed to proceed under O_2 atmosphere at the appropriate temperature. Aliquots were filtered through a small plug of silica gel (Et_2O eluent), evaporated, and analyzed by GC for conversion and chiral HPLC for alcohol ee.

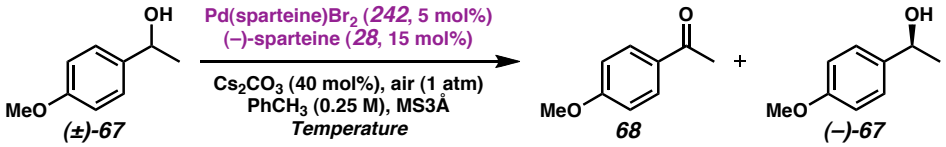

Kinetic Resolution Conditions with Pd(sparteine)Br_2 (242) and Air in $PhCH_3$. To an oven dried reaction tube with stir bar was added 3Å molecular sieves (250 mg). After allowing the tube to cool, Pd(sparteine)Br_2 (**242**, 12.5 mg, 0.025 mmol, 0.05 equiv) was added, followed by the $PhCH_3$ (1 mL) and then **28** (17.2 μL, 0.075 mmol, 0.15 equiv). A short (2-3 cm) tube containing Drierite was attached to the reaction tube. The reaction was warmed to the appropriate temperature (23 or 50 °C) and stirred vigorously

for 5 min. A solution of (±)-**67** (76.1 mg, 0.50 mmol, 1.0 equiv) and tridecane (36.6 μL, 0.15 mmol, 0.30 equiv) in $PhCH_3$ (1 mL) was added. The reaction was allowed to proceed under ambient air atmosphere at the appropriate temperature. Aliquots were filtered through a small plug of silica gel (Et_2O eluent), evaporated, and analyzed by GC for conversion and chiral HPLC for alcohol ee.

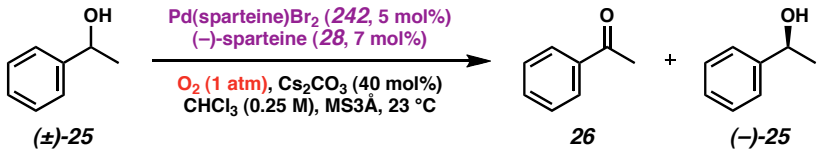

Kinetic Resolution Conditions with Pd(sparteine)Br_2 (242) and O_2 in $CHCl_3$. To an oven dried reaction tube with stir bar was added 3Å molecular sieves (250 mg). After allowing the tube to cool, **242** (12.5 mg, 0.025 mmol, 0.05 equiv) was added, followed by $CHCl_3$ (1 mL)[30] and then **28** (8.0 μL, 0.035 mmol, 0.07 equiv). The reaction tube was cooled to –78 °C, then vacuum evacuated and purged with O_2 (3x). The reaction was allowed to warm to 23 °C and stirred vigorously under a balloon of O_2 (1 atm) for 15 min. Finely powdered Cs_2CO_3 (65.2 mg, 0.20 mmol, 0.40 equiv) was added, followed by (±)-**25** (60.3 μL, 0.50 mmol, 1.0 equiv) and tridecane (36.6 μL, 0.15 mmol, 0.30 equiv) in $CHCl_3$ (1 mL). The reaction was allowed to proceed under O_2 atmosphere at 23 °C. Aliquots were filtered through a small plug of silica gel (Et_2O eluent), evaporated, and analyzed by GC for conversion and chiral HPLC for alcohol ee. Purification of the product ketone and enantioenriched secondary alcohol was accomplished by direct chromatography of the crude reaction mixture.

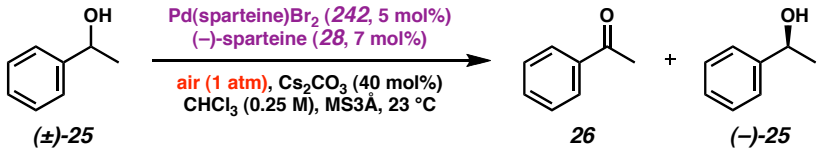

Kinetic Resolution Conditions with Pd(sparteine)Br_2 (242) and Air in $CHCl_3$. To an oven dried reaction tube with stir bar was added 3Å molecular sieves (250 mg). After allowing the tube to cool, **242** (12.5 mg, 0.025 mmol, 0.05 equiv) was added, followed by $CHCl_3$ (1 mL)[30] and then **28** (8.0 μL, 0.035 mmol, 0.07 equiv). A short (2-3 cm) tube containing Drierite was attached to the reaction tube. The reaction was stirred vigorously at 23 °C under a balloon of O_2 (1 atm) for 5 min. Finely powdered Cs_2CO_3 (65.2 mg, 0.20 mmol, 0.40 equiv) was added, followed by (±)-**25** (60.3 μL, 0.50 mmol, 1.0 equiv) and tridecane (36.6 μL, 0.15 mmol, 0.30 equiv) in $CHCl_3$ (1 mL). The reaction was allowed to proceed under ambient air atmosphere at 23 °C. Aliquots were filtered through a small plug of silica gel (Et_2O eluent), evaporated, and analyzed by GC for conversion and chiral HPLC for alcohol ee. Purification of the product ketone and enantioenriched secondary alcohol was accomplished by direct chromatography of the crude reaction mixture.

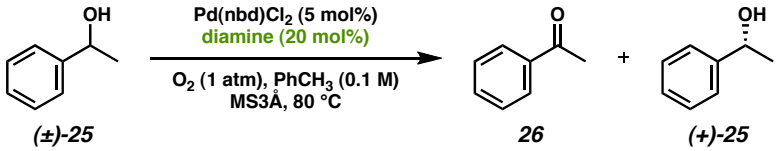

Kinetic Resolution Conditions With Diamines and Pd(nbd)Cl_2 in $PhCH_3$. To an oven dried reaction tube with stir bar was added 3Å molecular sieves (250 mg). After cooling, Pd(nbd)Cl_2 (6.7 mg, 0.025 mmol, 0.05 equiv) followed by toluene (2.5 mL) and then the diamine (0.10 mmol, 0.20 equiv) were added. The reaction tube was then cooled

to –78 °C, then vacuum evacuated and purged with O_2 (3x). Then, the tube was heated to 80 °C with vigorous stirring under a balloon of O_2 (1 atm) for 20 min. A solution of (±)-**25** (60.3 μL, 0.50 mmol, 1.0 equiv) and tridecane (36.6 μL, 0.15 mmol, 0.30 equiv) in toluene (2.5 mL) was added, and the reaction was allowed to proceed under O_2 atmosphere at 80 °C. Aliquots were filtered through a small plug of silica gel (Et_2O eluent), evaporated, and analyzed by GC for conversion and chiral HPLC for alcohol ee.

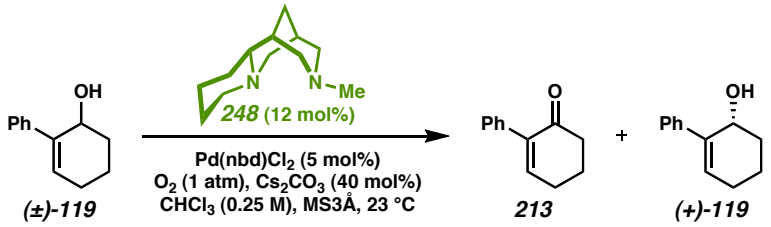

Kinetic Resolution Conditions With Diamine 248 and $Pd(nbd)Cl_2$ in $CHCl_3$. To an oven dried reaction tube with stir bar was added 3Å molecular sieves (250 mg). After allowing the tube to cool, $Pd(nbd)Cl_2$ (6.7 mg, 0.025 mmol, 0.05 equiv) was added, followed by $CHCl_3$ (1 mL)[30] and then freshly distilled diamine **248** (11.7 mg, 0.06 mmol, 0.12 equiv). The reaction tube was cooled to –78 °C, then vacuum evacuated and purged with O_2 (3x). The reaction was allowed to warm to 23 °C and stirred vigorously under a balloon of O_2 (1 atm) for 15 min. Finely powdered Cs_2CO_3 (65.2 mg, 0.20 mmol, 0.40 equiv) was added, followed by (±)-**119** (87.1 mg, 0.50 mmol, 1.0 equiv) and tridecane (36.6 μL, 0.15 mmol, 0.30 equiv) in $CHCl_3$ (1 mL). The reaction was allowed to proceed under O_2 atmosphere at 23 °C. Aliquots were filtered through a small plug of silica gel (Et_2O eluent), evaporated, and analyzed by GC for conversion and chiral HPLC for alcohol ee.

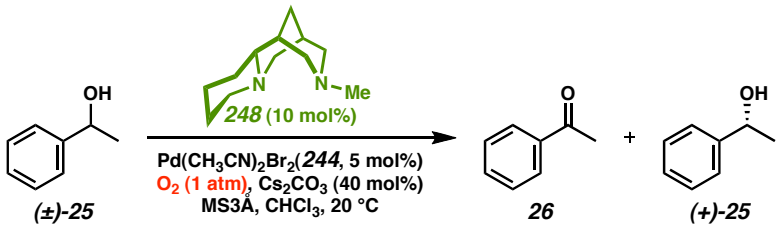

Kinetic Resolution Conditions with Pd(diamine)Br_2 and O_2. To an oven dried reaction tube with stir bar was added 3Å molecular sieves (250 mg). After allowing the tube to cool, **244** (8.7 mg, 0.025 mmol, 0.05 equiv) was added, followed by $CHCl_3$ (1 mL)[30] and then freshly distilled diamine **248** (9.7 mg, 0.050 mmol, 0.10 equiv). The reaction tube was cooled to –78 °C, then vacuum evacuated and purged with O_2 (3x). The reaction was warmed to 20 °C in a circulating bath and stirred vigorously under a balloon of O_2 (1 atm) for 15 min. Finely powdered Cs_2CO_3 (65.2 mg, 0.20 mmol, 0.40 equiv) was added, followed by (±)-**25** (60.3 μL, 0.50 mmol, 1.0 equiv) and tridecane (36.6 μL, 0.15 mmol, 0.30 equiv) in $CHCl_3$ (1 mL). The reaction was allowed to proceed under O_2 atmosphere at 20 °C. Aliquots were filtered through a small plug of silica gel (Et_2O eluent), evaporated, and analyzed by GC for conversion and chiral HPLC for alcohol ee. Purification of the product ketone and enantioenriched secondary alcohol was accomplished by direct chromatography of the crude reaction mixture.

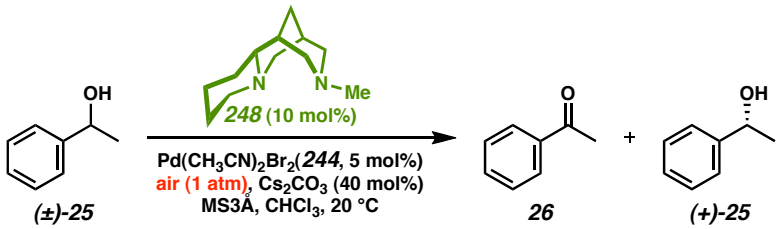

Kinetic Resolution Conditions with Pd(diamine)Br_2 and Air. To an oven dried reaction tube with stir bar was added 3Å molecular sieves (250 mg). After allowing

the tube to cool, **244** (8.7 mg, 0.025 mmol, 0.05 equiv) was added, followed by $CHCl_3$ (1 mL)[30] and then freshly distilled diamine **248** (9.7 mg, 0.050 mmol, 0.10 equiv). A short (2-3 cm) tube containing Drierite was attached to the reaction tube. The reaction was cooled to 20 °C in a circulating bath and stirred vigorously for 15 min. Finely powdered Cs_2CO_3 (65.2 mg, 0.20 mmol, 0.40 equiv) was added, followed by (±)-**25** (60.3 μL, 0.50 mmol, 1.0 equiv) and tridecane (36.6 μL, 0.15 mmol, 0.30 equiv) in $CHCl_3$ (1 mL). The reaction was allowed to proceed under ambient air atmosphere at 20 °C. Aliquots were filtered through a small plug of silica gel (Et_2O eluent), evaporated, and analyzed by GC for conversion and chiral HPLC for alcohol ee. Purification of the product ketone and enantioenriched secondary alcohol was accomplished by direct chromatography of the crude reaction mixture.

4.5.4 Preparative Resolution of Alcohols

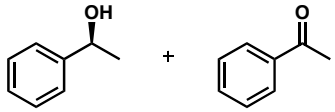

(–)-25 *26*

(–)-1-Phenylethanol ((–)-25, Table 4.2.11, entry 1). After 4 h (55.6% conversion), the crude reaction mixture was purified by flash chromatography (4:1 hexanes:Et_2O) to afford (–)-**25** (26.4 mg, 43% yield, 95.6% ee, s = 28) and **26** (28.5 mg, 47% yield, 91% total mass recovery).

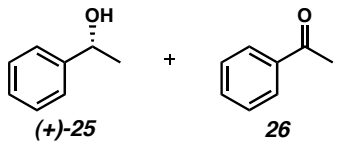

(+)-1-Phenylethanol ((+)-25, Table 4.3.6, entry 1). After 30 h (57.6% conversion), the crude reaction mixture was purified by flash chromatography (4:1 hexanes:Et_2O) to afford (+)-**25** (24.5 mg, 40% yield, 97.1% ee, *s* = 25) and **26** (30.8 mg, 51% yield, 91% total mass recovery).

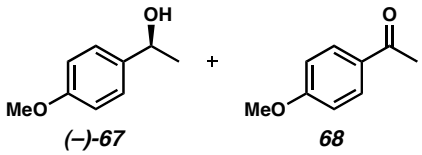

(–)-1-(4-Methoxyphenyl)ethanol ((–)-67, Table 4.2.11, entry 3). After 4 h (59.4% conversion), the crude reaction mixture was purified by flash chromatography (9:1→7:3 hexanes:EtOAc) to afford (–)-**67** (30.9 mg, 41% yield, 95.4% ee, *s* = 17) and **68** (43.3 mg, 58% yield, 98% total mass recovery).

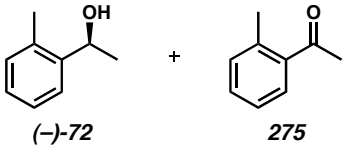

(–)-1-(2-Methylphenyl)ethanol ((–)-72, Table 4.2.11, entry 6). After 41 h (63.5% conversion), the crude reaction mixture was purified by flash chromatography (9:1→7:3 hexanes:EtOAc) to afford (–)-**72** (23.5 mg, 35% yield, 97.1% ee, *s* = 14) and **275** (33.2 mg, 50% yield, 84% total mass recovery).

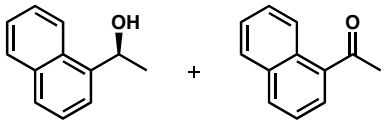

(–)-78 *276*

(–)-1-(1-Naphthyl)ethanol ((–)-78, Table 4.2.11, entry 8). After 24 h (59.6% conversion), the crude reaction mixture was purified by flash chromatography (9:1→7:3 hexanes:EtOAc) to afford (–)-**78** (34.2 mg, 40% yield, 92.5% ee, *s* = 14) and **276** (48.4 mg, 57% yield, 97% total mass recovery).

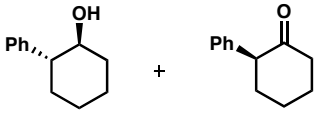

(+)-136 *(–)-277*

(+)-*trans*-2-Phenylcyclohexanol ((+)-136, Table 4.2.11, entry 12). After 49 h (58.0% conversion), the crude reaction mixture was purified by flash chromatography (19:1 hexanes:EtOAc) to afford (+)-**136** (34.9 mg, 40% yield, 90.6% ee, *s* = 15) and (–)-**277** (47.4 mg, 54% yield, 64.0% ee, 94% total mass recovery).

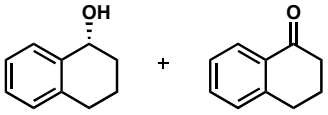

(–)-82 *278*

(–)-1-Tetralol ((–)-82, Table 4.3.6, entry 5). After 24 h (60.9% conversion), the crude reaction mixture was purified by flash chromatography (9:1→7:3 hexanes:EtOAc) to afford (–)-**82** (28.3 mg, 38% yield, 90.2% ee, *s* = 11) and **278** (39.0 mg, 53% yield, 92% total mass recovery).

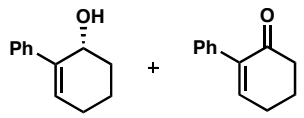

(+)-119 *213*

(+)-2-Phenylcyclohex-2-enol ((+)-119, Table 4.3.6, entry 6). After 46 h (56.8% conversion), the crude reaction mixture was purified by flash chromatography (19:1→4:1 hexanes:EtOAc) to afford (+)-**119** (37.6 mg, 43% yield, 90.7% ee, *s* = 17) and **213** (45.8 mg, 53% yield, 96% total mass recovery).

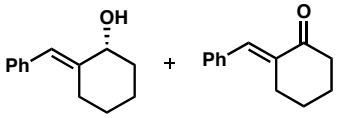

(+)-105 *279*

(+)-(*E*)-2-Benzylidenecyclohexanol ((+)-105, Table 4.3.6, entry 9). After 46 h (59.3% conversion), the crude reaction mixture was purified by flash chromatography (9:1 hexanes:EtOAc) to afford (+)-**105** (36.3 mg, 39% yield, 90.6% ee, *s* = 13) and **279** (51.2 mg, 55% yield, 94% total mass recovery).

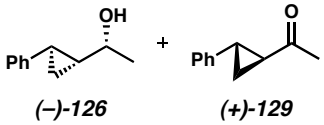

(–)-126 *(+)-129*

(–)-*syn*,*trans*-1-(2-Phenylcyclopropyl)ethanol ((–)-126, Table 4.3.6, entry 11). After 32 h (59.0% conversion), the crude reaction mixture was purified by flash chromatography (4:1 hexanes:EtOAc) to afford (–)-**126** (32.1 mg, 40% yield, 90.2% ee, *s* = 13) and (+)-**129** (42.3 mg, 53% yield, 64.1% ee, 92% total mass recovery).

4.5.5 Methods for Determination of Conversion

Conversion values for (±)-1-(9-anthacenyl)ethanol ((±)-**247**) were determined relative to product ketone by ^{1}H NMR of a reaction aliquot after filtration through a short plug of silica gel. All other conversions were determined by GC (Table 4.5.1 or Chapters 2 and 3) relative to tridecane as internal standard.

Table 4.5.1 Methods for determination of conversion.

entry	alcohol	ketone	GC conditions	alcohol retention time (min)	ketone retention time (min)
1	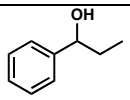 (±)-83	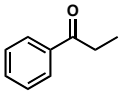 240	100 °C, 5 min; Ramp 13 °C/min	11.5	10.0
2	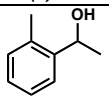 (±)-72	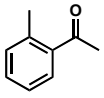 275	100 °C, 5 min; Ramp 13 °C/min	12.9	10.5
3	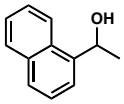 (±)-78	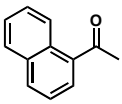 276	100 °C, 5 min; Ramp 13 °C/min to 240 °C 240 °C, 5 min	19.2	17.1
4	 (±)-136	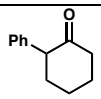 (±)-XX	100 °C, 5 min; Ramp 13 °C/min	14.2	14.9
5	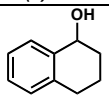 (±)-XX	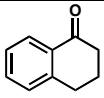 XX	100 °C, 5 min; Ramp 13 °C/min	14.5	13.6
6	 (±)-SI14	 (±)-277	100 °C, 5 min; Ramp 13 °C/min to 240 °C 240 °C, 5 min	15.8	16.1
7	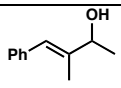 (±)-104	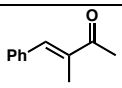 280	100 °C, 5 min; Ramp 13 °C/min	14.1	13.1

4.5.6 Methods for Determination of Enantiomeric Excess

Table 4.5.2 Methods for determination of enantiomeric excess.

entry	alcohol	ee assay and column	assay conditions	(*S*) enantiomer retention time (min)	(*R*) enantiomer retention time (min)
1	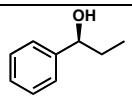 *(–)-83*	HPLC OD-H	3% EtOH/hexanes	17.6	12.0
2	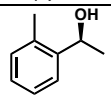 *(–)-72*	HPLC AD	3% EtOH/hexanes	13.1	11.2
3	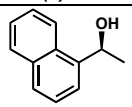 *(–)-78*	HPLC OD-H	8% EtOH/hexanes	12.6	18.4
4	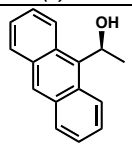 *(–)-247*	HPLC AD	5% EtOH/hexanes	17.6	27.9
5	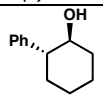 *(+)-136*	HPLC AD	4% EtOH/hexanes	28.1[a]	18.8
6	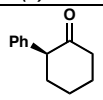 *(–)-277*	HPLC OB-H	3% EtOH/hexanes	18.1	23.2
7	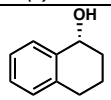 *(–)-82*	HPLC OB-H	3% *i*PrOH/hexanes	21.3	12.2
8	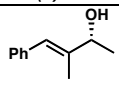 *(–)-104*	HPLC OD-H	3% *i*PrOH/hexanes	17.9	15.6

[a] Retention time for (*1S*, *2R*) enantiomer (shown).

4.6 Notes and References

(1) Portions of this chapter are reproduced in part from: Ebner, D. C.; Trend, R. M.; Genet, C.; McGrath, M. J.; O'Brien, P.; Stoltz, B. M. *Angew. Chem., Int. Ed.* **2008**, *47*, 6367-6370.

(2) (a) Nishimura, T.; Onoue, T.; Ohe, K.; Uemura, S. *Tetrahedron Lett.* **1998**, *39*, 6011-6014. (b) Nishimura, T.; Onoue, T.; Ohe, K.; Uemura, S. *J. Org. Chem.* **1999**, *64*, 6750-6755. (c) Nishimura, T.; Maeda, Y.; Kakiuchi, N.; Uemura, S. *J. Chem. Soc., Perkin Trans. 1* **2000**, 4301-4305. (d) Nishimura, T.; Uemura, S. *Synlett* **2004**, 201-216.

(3) Ferreira, E. M.; Stoltz, B. M. *J. Am. Chem. Soc.* **2001**, *123*, 7725-7726.

(4) The selectivity factor (*s*) was determined using the following equation: $s = \frac{\ln[(1-conv)(1-ee_{alc})]}{\ln[(1-conv)(1+ee_{alc})]}$, where ee_{alc} is the ee of the recovered alcohol and *conv* is the total conversion of alcohol to ketone, see: Kagan, H. B.; Fiaud, J. C. In *Topics in Stereochemistry*; Eliel, E. L., Ed.; Wiley & Sons: New York, 1988; Vol. 18, pp 249-330.

(5) Ferreira, E. M.; Stoltz, B. M. Unpublished results.

(6) Nielsen, R. J.; Keith, J. M.; Stoltz, B. M.; Goddard, W. A., III. *J. Am. Chem. Soc.* **2004**, *126*, 7967-7974.

(7) Kinetic studies performed by the Sigman group confirmed this finding, see: Mueller, J. A.; Jensen, D. R.; Sigman, M. S. *J. Am. Chem. Soc.* **2002**, *124*, 8202-8203.

(8) Trend, R. M.; Stoltz, B. M. *J. Am. Chem. Soc.* **2004**, *126*, 4482-4483.

(9) Mueller, J. A.; Sigman, M. S. *J. Am. Chem. Soc.* **2003**, *125*, 7005-7013.

(10) Bagdanoff, J. T. Development of the Enantioselective Oxidation of Secondary Alcohols and Natural Products Total Synthesis. Ph.D. Dissertation, California Institute of Technology, Pasadena, CA, 2005.

(11) Bagdanoff, J. T.; Stoltz, B. M. *Angew. Chem., Int. Ed.* **2004**, *43*, 353-357.

(12) Liu, H.; Liu, Y.; Zhu, C.; Liu, M.; Wang, C.; Chen, C.; Xi, F. *Synth. Met.* **1997**, *131*, 135-139.

(13) Trend, R. M.; Ramtohul, Y. K.; Ferreira, E. M.; Stoltz, B. M. *Angew. Chem., Int. Ed.* **2003**, *42*, 2892-2895.

(14) Raissa Trend also performed several preliminary oxidative kinetic resolutions utilizing Pd(sparteine)Br_2 (**242**) as catalyst in $CHCl_3$ and $PhCH_3$, obtaining results similar to Table 4.2.7, entry 5, and Table 4.2.9, entry 3, respectively.

(15) For dielectric constant tables, see: *CRC Handbook of Chemistry and Physics*, 76th ed.; Lide, D. R., Frederikse, H. P. R., Eds.; New York, 1995; Section 6, pp 159-192.

(16) Bagdanoff, J. T.; Ferreira, E. M.; Stoltz, B. M. *Org. Lett.* **2003**, *5*, 835-837.

(17) For a discussion of the limitations of conditions with Pd(sparteine)Cl_2 (**66**) in the oxidative kinetic resolution, see Chapter 3.

(18) For an asymmetric synthesis of (+)-sparteine, see: Smith, B. T.; Wendt, J. A.; Aubé, J. *Org. Lett.* **2002**, *4*, 2577-2579.

(19) Recently, similar palladium-catalyzed systems utilizing different ligands for enantioselective alcohol oxidation have been developed, see: (a) Jensen, D. R.; Sigman, M. S. *Org. Lett.* **2003**, *5*, 63-65. (b) Chen, T.; Jiang, J.-J.; Xu, Q.; Shi, M. *Org. Lett.* **2007**, *9*, 865-868. (c) Lesma, G.; Pilati, T.; Sacchetti, A.; Silvani, A. *Tetrahedron: Asymmetry* **2008**, *19*, 1363-1366.

(20) Several achiral, monodentate amines and Pd(nbd)Cl_2 did not provide active catalysts for the oxidation of (±)-1-phenylethanol ((±)-**25**), see Chapter 2.

(21) O'Brien, P. *Chem. Commun.* **2008**, 655-667.

(22) Dearden, M. J.; Firkin, C. R.; Hermet, J.-P. R.; O'Brien, P. *J. Am. Chem. Soc.* **2002**, *124*, 11870-11871.

(23) Dixon, A. J.; McGrath, M. J.; O'Brien, P. *Org. Synth.* **2006**, *83*, 141-154.

(24) Dearden, M. J.; McGrath, M. J.; O'Brien, P. *J. Org. Chem.* **2004**, *69*, 5789-5792.

(25) Johansson, M. J.; Schwartz, L.; Amedjkouh, M.; Kann, N. *Tetrahedron: Asymmetry* **2004**, *15*, 3531-3538.

(26) Heyari, A.; Mehrdad, M.; Maleki, A.; Ahmadi, N. *Synthesis* **2004**, 1563-1565.

(27) Genet, C.; McGrath, M. J.; O'Brien, P. *Org. Biomol. Chem.* **2006**, *4*, 1376-1382.

(28) Drew, D.; Doyle, J. R. *Inorg. Synth.* **1972**, Vol. XIII, 53-55.

(29) Grant, T. N.; West, F. G. *J. Am. Chem. Soc.* **2006**, *128*, 9348-9349.

(30) $CHCl_3$ stabilized with amylenes. $CHCl_3$ stabilized with EtOH must be distilled prior to use.

(31) Phenoxide was prepared by adding Na (1.0 equiv) to the appropriate phenol (1.05 equiv) in $PhCH_3$ (0.1 M). After the Na was consumed, the mixture was concentrated under reduced pressure and used without further purification.

(32) For conditions with Pd(sparteine)Br_2, 7 mol% (–)-sparteine (**28**) was added.